MEASURING THE SPATIAL CORRELATION BETWEEN TEMPERATURE AND VULNERABILITY ACROSS THE URBAN ENVIRONMENT

A Thesis
Presented to
The Academic Faculty

By

Kaitlin Morano

In Partial Fulfillment
of the Requirements for the Degree
Master of City and Regional Planning in the
School of City and Regional Planning

Georgia Institute of Technology

December 2014

MEASURING THE SPATIAL CORRELATION BETWEEN TEMPERATURE AND VULNERABILITY ACROSS THE URBAN ENVIRONMENT

Approved by:

Dr. Steven French, Advisor
School of City and Regional Planning
Georgia Institute of Technology

Dr. Brian Stone
School of City and Regional Planning
Georgia Institute of Technology

Dr. Subhrajit Guhathakurta
School of City and Regional Planning
Georgia Institute of Technology

ACKNOWLEDGEMENTS

First and foremost, thank you to the members of my committee, each of whom has helped guide me through this process and has been a fantastic mentor throughout my time at Georgia Tech. I am profoundly grateful for their time, interest, and advice—both thesis-related and otherwise—over the past two years.

Thank you to Dr. Bob Oliver, who shared with me his passion for geography, taught me to think critically about cities, engaged me with honest perspectives on academic life, and first introduced me to urban heat islands.

I'd also like to thank my friends and colleagues in the School of City and Regional Planning and elsewhere, whose humor, kindness, and encouragement have made many late nights (and early mornings … and late nights …) at school significantly more enjoyable.

I am incredibly thankful for my family, who are and always have been my greatest source of love and inspiration.

Lastly, my sincere thanks to Matt Reyburn, whose patience, support, and sacrifice have meant the world to me. I could not have done this without him.

TABLE OF CONTENTS

ACKNOWLEDGEMENTS III

TABLE OF CONTENTS IV

LIST OF TABLES VII

LIST OF FIGURES VIII

SUMMARY IX

INTRODUCTION 1

1.1 Context 1

1.2 Importance 4

1.3 Study Summary 5

LITERATURE REVIEW 8

2.1 Urban Heat Islands 8

2.1.1 Physical Foundations of the Urban Heat Island 11

2.1.2 Land Surface Determinants of the Urban Heat Island 17

2.1.3 Heat Island Measurement 19

2.2 Relationship Between Heat and Human Health 20

2.2.1 Morbidity 22

2.2.2 Mortality 23

2.3 Heat Vulnerability 24

2.3.1 Sociodemographic Characteristics of Heat Vulnerability 26

2.3.2 Environmental Characteristics of Heat Vulnerability 29

2.4 Limitations of Current Research 30

RESEARCH DESIGN 33

3.1 Research Question 33

3.2 Study Locations 34

3.3 Data 37

3.3.1 Air and Surface Temperature 37

3.3.2 Heat Vulnerability 39

3.4 Methodology 40

3.4.1 Air Temperature 41

3.4.2 Heat Vulnerability Index 52

3.4.3 Spatial Correlation of Temperature and Vulnerability 59

RESULTS 61

4.1 Air Temperature 61

4.1.1 Spatial Regression 63

4.1.2 Geostatistical Interpolation 65

4.2 Heat Vulnerability 69

4.2.1 Sociodemographic and Environmental Vulnerability 69

4.2.2 Principal Components Analysis 71

4.2.3 Spatial Autocorrelation of Vulnerabilities 76

4.3 Spatial Correlation 81

RECOMMENDATIONS 85

5.1 A Comprehensive Approach to Heat Vulnerability 86

5.1.1 Understanding the Interactions between Elements of Vulnerability 86

5.2 Strategies to Manage Urban Heat And Environmental Vulnerability 87

5.2.1 Urban Greening 89

5.2.2 Increasing the Albedo of Urban Surfaces 92

5.3 Strategies to Address Sociodemographic Vulnerability to Heat 94

5.4 Introducing a Spatial Component into Heat-Health Vulnerability 95

CONCLUSION 97

6.1 Summary of Findings 97

6.2 Future Work 98

REFERENCES 101

LIST OF TABLES

Table 1: Comparision of the Cities of Atlanta and Minneapolis 36

Table 2: Estimated Ground Surface Emissivity by NDVI Range.....46

Table 3: Scheme for Recoding Land Cover Classes 55

Table 4: Descriptive Statistics for Air Temperature Prediction Variables 63

Table 5: Results of Spatial Regression.....65

Table 6: Summary of Co-Kriging Models 66

Table 7: Descriptive Statistics for Vulnerability Variables.....70

Table 8: Correlation between Vulnerability Variables 72

Table 9: Results of Principal Components Analysis 73

LIST OF FIGURES

Figure 1: Profile of the Urban Heat Island Effect 9

Figure 2: Effects of Urbanization on the Surface Energy Balance 16

Figure 3: Health Consequences of Heat 21

Figure 4: Societal and Environmental Determinants of Risk 25

Figure 5: Cities of Atlanta and Minneapolis 35

Figure 6: Correlation between NCDC and Weather Underground Stations 39

Figure 7: Satellite Image Processing Model 42

Figure 8: Variables used to Estimate Air Temperature 62

Figure 9: Heat Vulnerability Index for Atlanta 75

Figure 10: Heat Vulnerability Index for Minneapolis 3675

Figure 11: Most and Least Vulnerable Block Groups 77

Figure 12: Spatial Autocorrelation of Vulnerability Components for Atlanta 78

Figure 13: Spatial Autocorrelation of Vulnerability Components for Minneapolis 80

Figure 14: Spatial Correlation between Vulnerability and Temperature in Atlanta 82

Figure 15: Spatial Correlation between Vulnerability and Temperature in Minneapolis . 83

SUMMARY

This thesis is concerned with a challenge lying at the intersection of urbanization and climate change. As global temperatures rise, cities both amplify that warming and contribute to it. Therefore, as cities prepare to accommodate an increasing majority of the world's population, the consequences of a warming climate are becoming exceedingly critical. Accordingly, urban locales have become the ideal platform from which to address the issue of climate change and, specifically, its implications for human health.

The purpose of this work is to examine the spatial correlation between elevated temperatures and populations most vulnerable to heat across the urban environment. Building on previous studies that have focused primarily on either the physical determinants of hot spots or the spatial distribution of heat-vulnerable populations, this research measures the extent to which these two phenomena are co-located on a smaller scale. Introducing an explicit spatial component into the analysis will afford municipalities greater precision in deploying resources and implementing strategies to improve the health of city residents.

The relationship between local hot spots and vulnerability to heat is investigated in the cities of Atlanta, Georgia and Minneapolis, Minnesota using a three-part approach.

First, satellite imagery and ground observations are used to estimate continuous air temperature across the urban environment. A heat vulnerability index is then derived from sociodemographic and environmental variables at the Census block group level. Finally, a spatial statistical analysis is performed to identify the areas with both the hottest temperatures and the most vulnerable populations.

In both Atlanta and Minneapolis, a moderately strong relationship is found between elevated temperatures and populations most vulnerable to heat. This is especially true in particular locations in each city, corroborating the benefit afforded by an explicit consideration of place. Furthermore, distinct spatial patterns are observed between sociodemographic, environmental, and comprehensive heat vulnerability, suggesting conventional inquiries to identify the location of vulnerable populations that do not consider environmental components may be inaccurate. Specific suggestions for reducing urban temperatures and environmental vulnerability are offered, as well as ones for addressing sociodemographic vulnerability throughout the urban environment. Finally, the study concludes with recommendations, based on these findings, to consider vulnerability to heat comprehensively and to incorporate a spatial component into future analyses.

CHAPTER I

INTRODUCTION

As the twenty-first century begins, two discrete yet distinctly intertwined phenomena of paramount importance have emerged: urbanization and climate change. Because of this connection, it is vital to address each of these processes concurrently, but to do so successfully also requires an understanding of the complex relationships that exist between them. In this respect, the co-evolutionary nature of urban growth and climate change presents significant opportunities to examine how these processes interact; how that reciprocal interaction will impact society; and, ultimately, what role humans have in influencing such outcomes.

1.1 CONTEXT

Global climate change is arguably the single-most critical challenge facing humans today. Having achieved near complete consensus among climate researchers and academics, little doubt exists within the scientific community as to the transformation of Earth's climate currently underway. Indeed, both long-term warming trends and the rate at which those trends have accelerated in recent decades are directly observable in the climatic record. Less

conspicuous, however, is the divergent manner in which this rise in temperature is occurring: at the global scale, warming results from an accumulation of greenhouse gases in the atmosphere; at the local scale, however, the warming of cities is predominantly driven by changes in land cover. The division between these spatial scales does not imply that the two processes are mutually exclusive; rather, it highlights the interconnectedness of the natural and built environments and their sensitivities to one another. As the global urban population grows, an understanding of the spatiality of these climatic processes—particularly at the local scale—and how they will affect urban populations becomes increasingly important.

As of 2008, more than 50% of the global population resides in cities [69]. This amount is projected to increase into the future: according to the United Nations Development Programme (2011), the urban proportion of Earth's population will rise to 70% by 2050. While a large majority of this growth is expected to occur in developing regions with neither the financial nor technical resources to manage such rapid change, the urban population in the United States is also predicted to increase during this period [69].

As new development occurs to accommodate this population influx, however, the built environment will be altered in a way that significantly affects the physical environment surrounding it. The replacement of open, vegetated land with the surfaces that characterize

urban settlements modifies the local temperature and moisture characteristics of an area, contributing to a climatological phenomenon known as the urban heat island effect.

The primary contributing factor to heat island formation is land cover change. On rural or underdeveloped land, vegetation plays a significant role in moderating air temperature by performing evapotranspiration—a natural cooling process whereby incoming solar radiation is captured and its energy used to convert water into water vapor. The vegetative cover performing this cooling process is not simply eliminated during development of the built environment, it is replaced with vast amounts of impervious surfaces, many of which are characterized by low reflectivity and a remarkable ability to absorb and retain heat. The augmentation of settlements and significant escalation of land cover change that will inevitably accompany urban growth suggests much warmer futures for city-dwellers around the globe.

The fact that cities exhibit warmer temperatures relative to the non-urban areas at their periphery becomes increasingly important because, as global temperatures continue to rise, urban areas both amplify that warming and contribute to it. In fact, many cities in the United States are warming at twice the rate of Earth as a whole, yet little attention is paid to local climate processes [67]. Nevertheless, exposure to increased temperatures signifies important consequences for public health, air and water quality, and energy consumption for many ill-prepared municipalities even in the United States.

Heat islands exist, in essence, at the nexus of urbanization and climate change; they represent the direct, physical manifestation of warming temperatures within cities themselves. Although urban areas cover approximately 3% of Earth's surface, more than 50% of the global population is concentrated in these locales. Accordingly, cities have become the optimal platform from which to address the issue of climate change and, specifically, its implications for human health.

1.2 IMPORTANCE

Each year, extreme heat is more costly to human life than hurricanes, tornadoes, earthquakes, floods, and lightning combined [44]. This is magnified in urban areas, where stagnant air traps pollutants and already-elevated temperatures are often exacerbated by high humidity. Unfortunately, heat warnings are largely unheeded by the general public, yet the extensive fatalities and from recent extreme heat events are difficult to ignore: at least 700 deaths occurred as a result of the 1995 Chicago heat wave [31, 53]; mortality estimates range between 52,000 and 70,000 from the heat wave in Europe during the summer of 2003 [50]; and nearly 15,000 lives were claimed by a heat wave across Russia in 2010 [10].

In the United States, extreme heat has also had a profound impact on outdated infrastructure and transportation systems. Perhaps the most well-known example of this influence occurred on August 14, 2003: an increase in energy demand for cooling—caused by

elevated temperatures in the region—exceeded the capacity of New York's power grid, eventually causing it to automatically shut down. The resulting blackout affected more than 50 million people across the Northeast and Midwest and into Canada, and cost an estimated $6 to $10 billion [12].

Elevated temperatures also pose a distinct problem to the aging population in the United States. As the human body grows older, its ability to withstand the negative health effects associated with thermal stress is greatly diminished. Furthermore, the increased prevalence of cardiovascular disease, diabetes, and obesity—all diseases that decrease the adaptive capacity of the human body to heat—indicates a growing number of Americans are becoming increasingly vulnerable to heat illness and heat death. As such, municipalities must simultaneously contend with the unique public health challenges that accompany a shift in both population characteristics and geography, in concert with a warming climate.

1.3 STUDY SUMMARY

This thesis aims to examine the spatial relationship between elevated air temperatures and populations most vulnerable to heat across the urban environment. Previous studies have largely focused either on heat island intensity and the physical determinants of urban heat islands, or on the spatial distribution of heat-vulnerable populations. This analysis at-

tempts to further the existing research by exploring the co-location of local heat island intensity and comprehensive vulnerability to heat. The study will focus on Atlanta, Georgia and Minneapolis, Minnesota.

These cities were selected due to several key traits—both mutual and exclusive—that may facilitate comparison and engender more valuable conclusions. For example, while both cities have similarly-sized populations, the population density of Minneapolis is more than double that of Atlanta. This undoubtedly has significant implications for urban form and, consequently, heat island formation. Also, the cities are located in two very different geographic regions of the country. A comparison of the results can help determine whether or not the spatial relationship between elevated temperatures and vulnerability to heat is independent of variations in regional climate.

A three-part methodology will be employed in this analysis: first, continuous air temperature will be estimated using satellite imagery and weather station observations; second, a heat vulnerability index will be generated based on demographic, social, and environmental variables; and third, a spatial statistical analysis will be performed to measure the co-location between the hottest air temperatures and the populations most vulnerable to heat.

As municipalities and local governments plan for a future with warmer temperatures and larger urban populations, effective policies must be designed with respect to both the

social and physical environments. The results of this analysis can help inform such strategies. Finally, this thesis concludes with policy recommendations that attempt to address the comprehensive nature of vulnerability in relation to extreme heat across the urban environment.

CHAPTER II

LITERATURE REVIEW

This chapter seeks to establish a foundation on which this work intends to build and presents a review of the existing literature of several fields relevant to this study. The following discussion is focused on urban heat islands; the relationship between heat and human health; and the characteristics of sociodemographic and environmental heat vulnerability.

2.1 URBAN HEAT ISLANDS

Driven by land cover change, the geometric attributes of high density development, and anthropogenic waste heat emissions, the urban heat island effect is "emerging to be the principal climate-related threat to human health today" [57, p. 74]. Together, these factors cause cities to experience warmer temperatures than nearby, non-urban and rural areas (Figure 1).

Generally, heat islands are grouped into two distinct categories: surface heat islands and atmospheric heat islands [68]. Surface heat islands are simply the elevation in temperature of surfaces in urban areas over surfaces in the surrounding rural areas. This type of

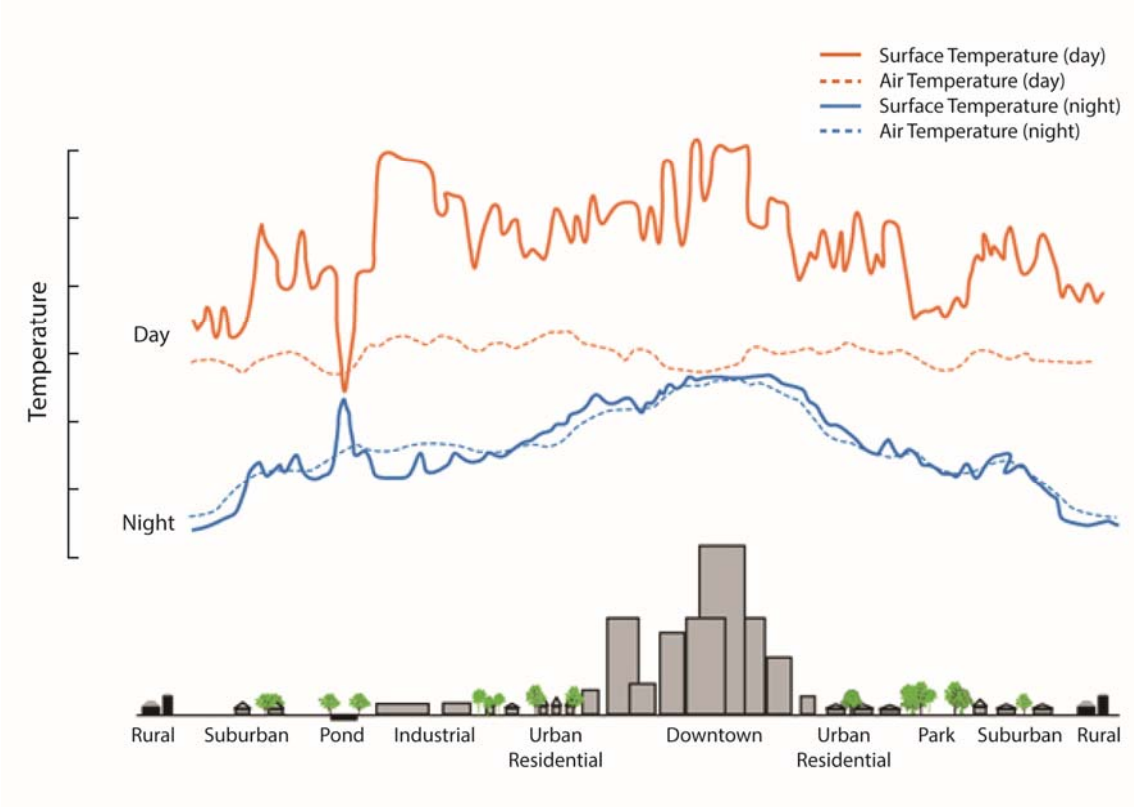

Source: adapted from US EPA, http://www.epa.gov/heatisland/images/UHI_profile-rev-big.gif

Figure 1: Profile of the Urban Heat Island Effect

heat island may be measured indirectly using remote sensing technologies to measure radiant thermal emissions from urban locations. Surface heat islands are present at all times, but are often most intense during the day when urban materials receive the most solar radiation. Additionally, surface heat islands are not heavily influenced by the anthropogenic heat sources that affect the air temperature of a city, such as transportation vehicles or heating and cooling units. Given the fluid characteristics of the atmosphere, the potential variability in temperature at any given elevation, and the general scarcity of temperature monitoring stations throughout cities, surface temperature is often used as an indicator of

an area's thermal attributes despite the fact that it is not a direct measure of air temperature. Still, "strong evidence exists that there is a significantly positive relationship between the surface and ambient air temperature" [28, p. 24].

Atmospheric heat islands, on the other hand, are the elevation in near-surface (12 meters) air temperature of an urban area over that of nearby rural areas. These heat islands are monitored with temperature measurements taken directly and simultaneously at various points throughout a city. Often, they may not be present during the day and are most intense at night due to a gradual release of heat from urban surfaces and water bodies. Because the human body regulates internal temperature during the evening when cooler air is generally present, the nocturnal intensity of atmospheric heat islands engenders the most dangerous and direct impacts on human health.

A basic understanding of the complex physical processes that govern local climate is essential in order to better comprehend the formation of urban heat islands and how they relate to land cover and, thus, urban growth. In this regard, of particular importance to this work is the connection between surface and atmospheric temperatures. In the subsequent sections, a brief overview of the Earth-atmosphere energy balance and energy transfer mechanisms is given, followed by an examination of existing literature on the land surface determinants of urban heat islands.

2.1.1 Physical Foundations of the Urban Heat Island

2.1.1.1 Earth-Atmosphere Energy Balance

Studies concerning the manner in which Earth's atmosphere interacts with inbound and outgoing radiation assume the sun emits radiation as a perfect blackbody. In theoretical physics, a blackbody is both an 'ideal' and 'diffuse' emitter of radiation: it emits radiation isotropically, according to temperature, regardless of the surface properties or composition of the blackbody itself [14]. Although emitted throughout the electromagnetic spectrum, solar radiation peaks in the visible subsection of the spectrum with comparatively shorter wavelengths; Earth, on the other hand, simply approximates a blackbody, and its emitted radiation peaks at longer wavelengths. This is an important quality governing the way in which Earth's atmosphere interacts with both solar and terrestrial radiation.

Earth's atmosphere selectively interacts with incoming solar radiation in one of three ways. These include reflection, transmission, and absorption. The mechanism through which radiation is processed largely depends on the wavelength of the radiation itself, as well as the composition of gases in Earth's atmosphere. Incoming solar radiation in the visible spectrum is transmitted through the atmosphere to Earth's surface, while the remainder is either reflected back out to space or selectively absorbed by atmospheric gases. The overall share of radiation that is reflected, transmitted, or absorbed by atmospheric gases and Earth's surface is known as the Earth-atmosphere energy balance [55]. The term 'balance'

is drawn from the first law of thermodynamics, which dictates energy in an isolated system can be neither created nor destroyed, rather it can only change forms. Accordingly, the amount of energy entering Earth's system must be roughly equal to the amount of energy leaving the system on an annual basis [14].

Shortwave radiation that is transmitted through the atmosphere and reaches Earth's surface can then either be reflected or absorbed by surface materials. In contrast to the manner in which solar radiation is handled in the upper atmosphere—determined largely by wavelength—the mechanism used to manage radiation at Earth's surface is determined by the properties of the surface itself. Namely, the albedo, or reflectivity, of a surface dictates the amount of solar radiation that will be reflected back into the atmosphere [42]; in this way, albedo ultimately dictates the amount of radiation that will be absorbed by Earth's surface as well.

2.1.1.2 Heat Transfer Mechanisms

2.1.1.2.1 Radiation

Once absorption of solar radiation occurs at Earth's surface, it can affect the near-surface air temperature through one of four heat transfer mechanisms [14]. The first of these energy transfer mechanisms is radiation. This occurs when incoming shortwave solar radiation, absorbed by Earth's surface, is re-emitted at longer wavelengths in the far-infrared section of the electromagnetic spectrum. As previously mentioned, because the gaseous

constituents of Earth's atmosphere absorb and transmit radiation selectively—in general, longwave radiation is absorbed and shortwave radiation transmitted—wavelength has significant implications for the amount of radiant energy in the atmosphere at any given time. In fact, the reemission of longwave radiation and the subsequent selective absorption by atmospheric gases is the underlying cause of a global increase in temperature widely known as the greenhouse effect [57].

The efficiency of the radiative process is governed by the emissivity of materials on Earth's surface. In this respect, changes in land cover that impact the ability of a surface to re-emit radiation directly affect the amount of longwave radiation in—and, consequently, temperature of—the atmosphere.

2.1.1.2.2 Conduction

The second mechanism of heat energy transfer is conduction, which occurs when heat energy is transferred between static materials of differing temperature that are in direct contact with one another. As energy is received by an object, the average kinetic energy of that object's molecules will increase—thus, raising its temperature. Molecular collisions at the boundary between this object and a cooler one serve to transfer heat energy from the warmer to the cooler object [14]. The role of conduction in heat island formation, however, is limited. "Although some level of conduction does take place between the ground and air immediately above, the primary role of conduction in heat island formation concerns the

distribution of heat energy within the solid construction materials of urbanized regions" [55, p. 26]. This is due to the physical properties and composition of atmospheric gases; with comparatively low molecular density and a rather fluid quality, gaseous materials are poor conductors of thermal energy.

2.1.1.2.3 Convection

A third mechanism of heat energy transfer is convection, whereby energy passed from a warmer object to a cooler (liquid or gaseous) one causes the cooler object to warm, rise, and expand. As convection occurs, the cooler object's molecules increase in kinetic energy and the object becomes more buoyant, causing it to rise. At higher altitudes with lower pressure, thermal expansion occurs, and heat is dissipated into the atmosphere; this process is known as adiabatic cooling. It is largely through convection that changes in land cover most significantly affect local air temperature. This concept is more thoroughly examined in Section 2.1.1.3.

2.1.1.2.4 Evaporation

The fourth mechanism of heat energy transfer, evaporation, is slightly different from radiation, conduction, and convection in that it involves the physical exchange of molecules between materials, and thus transfers energy between open systems [14]. Specifically, evaporation is a natural cooling process whereby inbound radiant solar energy is used to convert water into water vapor. As water vapor molecules rise to higher altitudes, they condense to

form water droplets and, eventually, clouds. During this condensation process, heat energy is released back into the atmosphere, warming the atmospheric temperature at higher altitudes.

2.1.1.3 Repartitioning of the Surface Energy Flux

The connection between surface and atmospheric heat exchange as it relates to urban heat islands is based upon the way in which heat is transported from Earth's surface to the atmosphere: either as sensible or latent heat [55]. Sensible heat is that which is experienced by humans as discernible increases in air temperature—the process of convection produces sensible heat. When an air parcel experiences adiabatic lifting and cooling, the heat continuously lost from that parcel as it rises dissipates into the atmosphere, warming the air and causing an increase in local near-surface temperature.

Latent heat, on the other hand, is that which is not detected by humans because it does not contribute to increased air temperatures near Earth's surface—evaporation introduces latent heat into the atmosphere [57]. As solar radiation is used to turn water into water vapor, thermal energy remains encapsulated in the water vapor as it rises, and it is only released into Earth's atmosphere when the water vapor particles condense back into water droplets at higher altitudes. Because the amount of energy in a system must be in balance, the amount of latent heat energy necessarily limits the amount of sensible heat energy available. Thus, an increase in local temperature is directly related to the relative

amount of convection (producing sensible heat) and evaporation (producing latent heat) occurring in an area.

Accordingly, the urban heat island effect can be defined as a repartitioning of the surface energy balance, driven by land cover changes associated with urbanization, resulting in an augmentation of the sensible heat flux and a reduction of the latent heat flux over that which occurs in the natural environment (Figure 2) [42, 57].

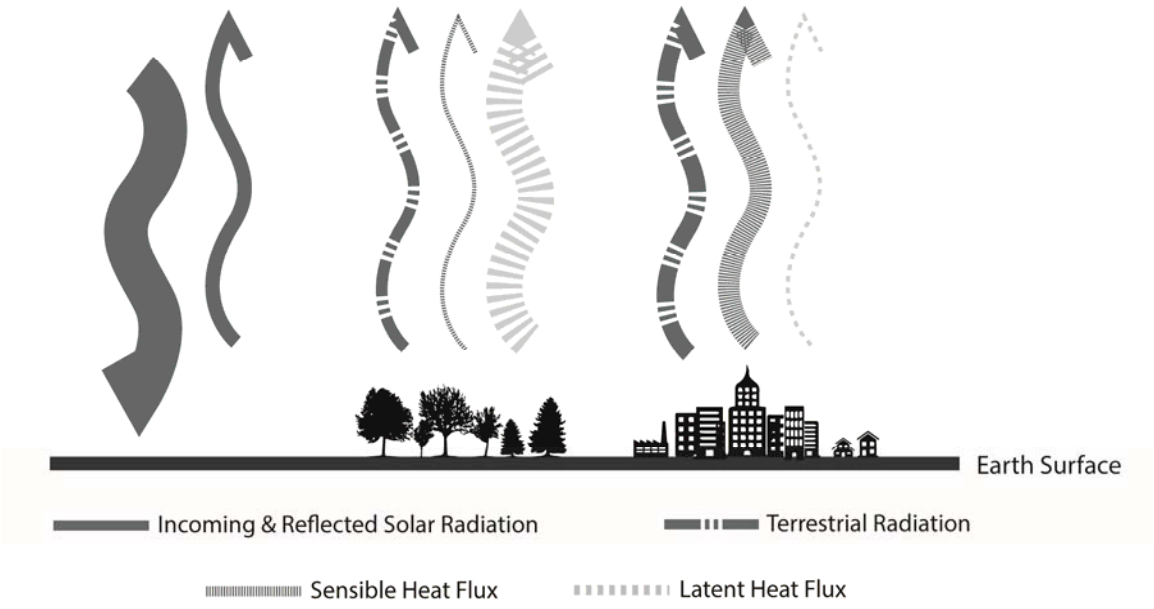

Source: adapted from Stone (2012)

Figure 2: Effects of Urbanization on the Surface Energy Balance

Engendered by the built environment, this reapportionment of surface energy between fluxes significantly alters the type of heat present in the atmosphere and, therefore,

local air temperature. By decreasing the amount of vegetative cover performing evapotranspiration and increasing the amount of materials with low albedo and high thermal capacity, the physical attributes of a city have been shown to increase longwave terrestrial radiation and forcibly modify both local and regional climates [56].

2.1.2 Land Surface Determinants of the Urban Heat Island

A considerable amount of literature has been published on ways in which the properties of Earth's surface affect local climate and, specifically, the formation and magnitude of heat islands. In fact, changes to the land surface are believed to influence climate to approximately the same degree as anthropogenic greenhouse gas emissions [13]. As discussed above, the mechanism with which a material transfers thermal energy is of paramount importance in determining the type of heat produced. In his influential work, Oke (1987) sums,

> *The process of urbanization produces radical changes in the nature of the surface and atmospheric properties of a region. It involves the transformation of the radiative, thermal, moisture and aerodynamic characteristics and thereby dislocates the natural solar and hydrologic cascades. (p. 240)*

Just as all surfaces do not interact with solar radiation in precisely the same way, not all land covers have equal effect on Earth's climate. Chief among the surface properties that influence local heat flux are albedo and thermal capacity [42]. Albedo is dependent upon

surface roughness and color. Whereas smooth, light-colored materials—such as undisturbed snow and ice—reflect more incident solar radiation and have a higher albedo, rough, dark-colored materials—such as asphalt and brick—reflect less incident solar radiation and have a lower albedo. Furthermore, the materials used in the construction of cities typically have a higher thermal capacity than that of the natural environment; with the exception of water, which has an exceptionally high heat capacity but is generally not replaced in favor of the construction of urban settlements, these materials have a greater ability to store and retain heat more effectively. Together with tall buildings that prevent the full departure of outgoing radiation, the low albedo and high thermal capacity of urban surfaces cause cities to absorb and retain more heat energy than non-urban landscapes [42].

Because changes in land cover have such significant impacts on local climate, "certain areas of a city might experience episodes of extreme heat while other areas within the city, only a few hundred meters away, would not approach the same extreme heat threshold" [28, p. 24]. This ultra-localized manifestation of the heat island effect implies that hotter temperatures can be experienced on a much smaller, perhaps sub-neighborhood scale; this is an important underlying premise of this thesis.

Overall, replacement of the natural landscape with the materials that characterize urban settlements not only alters the albedo and thermal capacity of Earth's surface [42], it reapportions the natural surface energy balance. These local urban influences are often

overlooked, however, in Global Climate Models due to the fact that cities cover only 3% of Earth's surface. This oversight has caused the role of land cover change and urban heat islands to be underestimated in predictions of future climate [57].

2.1.3 Heat Island Measurement

Several different approaches to measuring the urban heat island effect exist throughout the surveyed literature. The methods employed depend largely on the type of heat island being assessed—as such, measurement techniques may be grouped into two major categories: in-situ analyses and remote sensing analyses.

In-situ observations, used to evaluate atmospheric heat islands, are simply near-surface air temperature measurements taken directly and concurrently at various points or traverses throughout a city. In the early nineteenth century, a comparison of these ground temperature measurements between London and the rural land at its periphery led to perhaps the earliest record of the urban heat island effect [24]. Only including temperature values for discrete point locations in an analysis, however, necessarily restricts the accuracy and utility of atmospheric heat island measurement across space. Today, due to the spatial continuity and data precision afforded by widely-available satellite imagery, the exclusive use of in-situ observations in measuring urban heat islands is limited.

The application of remote sensing technologies to the analysis of surface heat islands provides a more comprehensive understanding of the urban climatological phenomenon than is granted by in-situ measurements alone. Moreover, it facilitates the indirect and simultaneous collection of data over expansive areas and at various spatial and temporal resolutions. Thermal infrared and multi-spectral satellite imagery has been of particular use in studying the thermal responses of different land cover types and their respective contribution to heat island formation [34]. Indeed, many studies have found associations between surface temperature and land use/land cover [68]. Given these simple surface temperature-land cover correlations and several assumptions regarding the density of different land uses, heat island growth has been successfully modeled as a function of changes in land cover over time [59, 47].

2.2 RELATIONSHIP BETWEEN HEAT AND HUMAN HEALTH

Recently, many studies in the public health discipline have focused on the relationship between temperature and health, with a substantial proportion of this research examining the health implications of climate change [35, 16, 15, 38, 17, 45]. Indeed, researchers have found a direct connection between human wellbeing and local temperature. The primary mechanism through which these two entities are linked is thermo-regulation: the ability of the human body to maintain an appropriate internal temperature regardless of the ambient,

external temperature surrounding it. As air temperature increases dramatically over the internal temperature of the human body, the capability of the body to dissipate heat and sustain normal functions—largely through perspiration—is decreased. Hotter temperatures can have grave consequences for human beings, eventually leading to heat stress, heat illness, and heat death (Figure 3) [33].

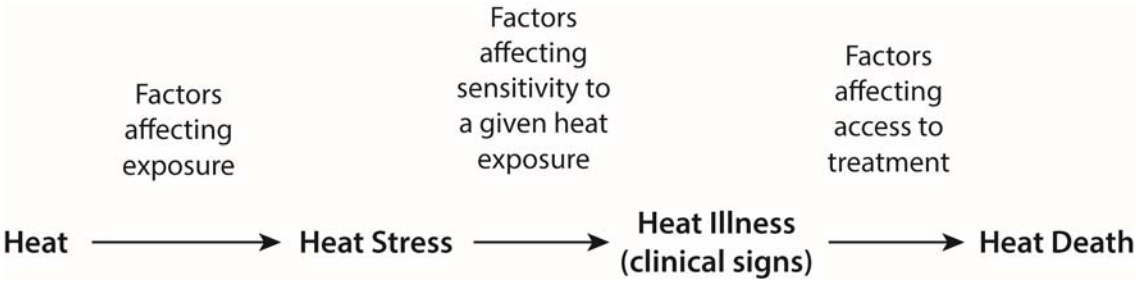

Source: Kovats and Hajat (2008)

Figure 3: Health Consequences of Heat

Increased heat exposure has been observed to increase morbidity and mortality, however this is not uniformly true, and varies according to the socioeconomic and demographic characteristics of a population as well as the environmental characteristics of a location [37, 65]. The specific attributes of population and place that affect heat vulnerability are discussed in Section 2.3; what follows herein is a summary of the heat-health relationship as it relates specifically to human morbidity and mortality.

2.2.1 Morbidity

It is likely that morbidity, defined as the incidence of disease or illness within a population, is directly augmented by increased temperatures. Comparatively fewer studies have explored heat-related morbidity relative to heat-related mortality. Still, it has been determined with very high confidence that increased temperatures "act [upon human health] mainly by exacerbating health problems that already exist" [54, p. 3].

Particularly during periods of intense heat, hospital admissions rise for heat exhaustion, heat stroke, heat cramps, heat syncope, and dehydration [33]; this is predominantly the case among individuals with nervous system disorders, respiratory diseases, and diabetes [52]. The same holds true, however, for individuals without preexisting conditions. A detailed study of the 1995 Chicago heat wave found that increased temperatures were responsible for approximately 11% excess admissions of all causes to local hospitals [53].

Rates of heat-exacerbated morbidity are amplified in individuals with preexisting cardiovascular, cerebro-vascular, renal, and respiratory diseases, as well as neurologic and behavioral disorders and mental illnesses [18, 19, 20, 32, 53]. It is possible that higher risk in individuals with preexisting conditions is due, at least in part, to prescribed medications that unintentionally inhibit the thermo-regulatory ability of the human body [36].

Moreover, Rhea (2012) observed several significant temperature thresholds to discretely affect heat-related morbidity:

> *Between 90°F and 98°F, the mean daily number of [heat-related illness emergency department] visits increased by 1.4 for each 1°F increase. In contrast, between 98°F and 100°F degrees, the mean daily number of [heat-related illness emergency department] visits increased by 15.8 for each 1°F increase. [p. 498]*

Although the relationship between increased temperatures and increased morbidity is not conclusive, evidence that prolonged heat exposure exacerbates preexisting illnesses and causes health-stress is growing. The relationship between heat and human mortality, however, is better defined.

2.2.2 Mortality

As the foremost cause of weather-related fatality in the United States, extreme heat is responsible for widespread loss of human life [35]. Because of the difficulty in verifying heat as the etiology of fatality, it is likely that the number of deaths directly attributable to elevated temperatures is underestimated [35]. Further, studies have shown the incidence of heat-related mortality in a population varies markedly according to geographic location—with heat being more detrimental to populations in the Northeast and Midwest than in the South and Southwest [35]. It has been argued that this geographic disparity is attributable to the acclimation of populations to regional climate variations [36].

Multiple extreme heat events in the past several decades have demonstrated the destructive power of elevated temperatures around the world: the 1995 Chicago heat wave was responsible for at least 700 deaths [31, 53]; mortality estimates from the summer 2003 heat wave in Europe range between 52,000 and 70,000 [50]; and a heat wave across Russia in 2010 claimed nearly 15,000 lives [10]. Recent work notes that higher temperatures during heat waves are amplified by the urban heat island effect, making extreme heat events exceedingly hazardous to city populations [66].

2.3 HEAT VULNERABILITY

A central aim of this work is to examine the spatial patterns of vulnerability across the urban environment; therefore, a foundational understanding of the term vulnerability is imperative. Specifying the concept of vulnerability as it relates to public health and climate change—and also how it differs from and relates to the terms risk and exposure—is essential in order to knowledgeably engage the current field of research. Additionally, a clear definition will facilitate more thorough assessment of the underlying causes, and ultimately impacts, of the spatial variation of vulnerability.

According to the Intergovernmental Panel on Climate Change (IPCC), vulnerability is broadly defined as "the propensity of exposed elements such as human beings … to suffer adverse effects when impacted by hazard events" [13, p. 69]. For this study, vulnerability is interpreted as a function of both the sensitivity of a population to heat and the capacity of

that population to cope with, recover from, and adapt to higher temperatures [54]. Correspondingly, exposure has been defined as "the presence of people, livelihoods, species or ecosystems, environmental functions, services, and resources, infrastructure, or economic, social, or cultural assets in places and settings that could be adversely affected" by increased heat [26, p. 4]. Coupled with the potential for hazardous temperatures to occur, interactions between vulnerability and exposure determine risk (Figure 4).

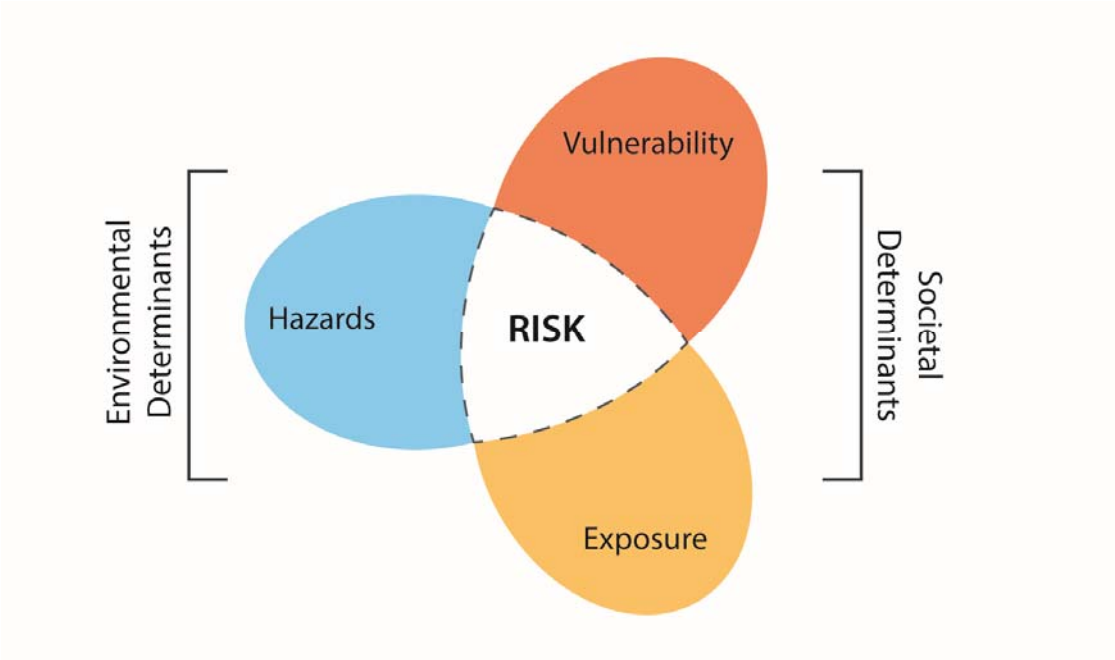

Source: adapted from the IPCC Fifth Assessment Report

Figure 4: Societal and Environmental Determinants of Risk

Risk has been defined by the IPCC as the "probability of occurrence of hazardous events or trends multiplied by the impacts if these events or trends occur" [6, p. 5]. In the

realm of this research, risk is understood to imply the possibility of a population experiencing negative health consequences from increased heat.

Of course, these elements of vulnerability are neither uniform throughout urban populations nor constant across urban environments. What is known is that, regardless of improved access to health care and public health facilities, urban populations are generally at higher risk—from both increased vulnerability and increased thermal exposures arising from the urban heat island—than their nearby rural counterparts [63]. A relatively small number of recent studies have attempted to delineate the spatial patterns of factors that influence heat vulnerability. Presented in the foregoing sections is a brief summary of this literature related to sociodemographic and environmental heat vulnerability, including the specific characteristics of population and place that exaggerate susceptibility.

2.3.1 Sociodemographic Characteristics of Heat Vulnerability

Throughout this work, the term "sociodemographic" vulnerability is used to represent a combination of social and demographic vulnerabilities. While social and demographic vulnerabilities are indeed similar, an important distinction exists among them. Principally, "demographic [vulnerabilities] are those related to individuals or the general population," while "social vulnerabilities describe differences for certain portions of the population that may make them more susceptible to extreme heat or less well equipped to deal with heat" [66, p. 193]. Elements of sociodemographic vulnerability in the context of

this study are those which pertain to or are directly influenced by human beings—either individually or collectively as a population.

Among the most widely-cited sociodemographic factors influencing an individual's vulnerability to heat are age, race, education, and poverty status [22, 25, 27, 48, 63, 66]. Elderly populations are extremely susceptible to the negative health consequences of heat, and exhibit a rise in both hospital admissions [32, 52] and heat-related deaths during periods of increased temperatures [48]. In fact, of the more than 400 average deaths attributed to heat each year, a majority of the deceased are over the age of 65 [4]. Additionally, due to the diminished or nonexistent capacity for independent mobility, both the very old and the very young are considered vulnerable to heat hazards [12].

Several different relationships have been found between race and the negative health outcomes of increased heat. A 1989 analysis of 48 cities across the United States observed a strong correlation between the percentage of nonwhite population and increased heat-related mortality in the South [29]. Likewise, in a vulnerability mapping study conducted by Reid et al. (2009) of the entire nation, the percentage of population per census tract identifying as a race other than white was found to contribute to increased vulnerability [48]. Yet another inquiry yielded slightly different results: in a 2008 case control study, the heat mortality rate was highest among the black population, second highest among the white population, and lowest among the Hispanic population [3].

Multiple scientific studies have found that educational achievement is correlated with heat mortality—specifically, individuals whose highest level of education is high school or below tend to experience higher rates of heat-related mortality than individuals who attended college or university [9, 43, 48].

There are several avenues through which poverty status is related to vulnerability and increased heat mortality. The first of these concerns properties of the built environment in low income areas: "in most urban areas, low income groups … face large climate change risks because of poor quality, insecure, and clustered housing, [and] inadequate infrastructure" [13, p. 8]. Similarly, the infrequence of air conditioning and central air ownership—or hesitation to utilize such amenities in anticipation of higher energy bills—in low income populations is significant because these cooling mechanisms are important components in preventing heat-death [48]. Finally, low income populations endure increased vulnerability through institutional and administrative deficiencies, such as "lack of provision for health care, emergency services … and measures for disaster risk reduction" [13, p. 8].

The rate of certain diseases is also a key indicator of the vulnerability of a population to heat. Most heat-related deaths during periods of increased temperatures have been shown to occur in individuals with preexisting cardiovascular and respiratory illnesses [18, 39]. Recent studies have revealed an increased vulnerability to heat in individuals diagnosed

with obesity [35] and diabetes as well [48]. As stated previously, the disease prevalence component of heat vulnerability may be partially due to the medications prescribed to these individuals, and therefore may not be completely attributable to the preexisting condition itself [36].

Another important sociodemographic characteristic that affects a population's vulnerability to heat is social isolation. The degree to which an individual interacts with others, has a reliable support network, and feels that they are able to reach out for aid or assistance greatly influences the risk of mortality from high ambient temperature. Often, this is measured for vulnerability mapping using a combination of proxy variables: household type (i.e., individuals living alone are generally more isolated than those in group quarters or communal living arrangements) [22, 48] and English language proficiency (i.e., individuals who lack the language skills to communicate effectively are less likely to ask for assistance during an emergency) [36, 63]. Studies show that during the Chicago heat wave of 1995, the level of a population's social isolation was directly correlated with the likelihood of fatality due to heat [31]. Additionally, analyses of the 2003 European heat wave show that, in France, one of the most significant risk factors for heat death was living alone [50].

2.3.2 Environmental Characteristics of Heat Vulnerability

The environmental factors that influence heat vulnerability in cities are similar to the land cover characteristics that affect local temperatures; mainly, these include amount of

vegetative cover and impervious surfaces within an area [22, 25, 63]. As discussed in Section 2.1, these land cover types are key determinants of how solar energy interacts with Earth's surface, and their variation can directly alter the surface energy flux, leading to hotter temperatures. In essence, then, environmental vulnerability is quite directly related to exposure [66]. Much agreement exists throughout the scientific literature that increased greenery and greenspace in an area is associated with lower temperatures in addition to decreased morbidity and mortality [25, 30, 61]. Impervious surfaces are partially responsible for raising local temperatures, contributing to formation of the urban heat island, and exacerbating heat waves; consequently, correlations between the amount of impervious surface cover in an area and the relative risk of heat-death have been observed as well [18].

2.4 LIMITATIONS OF CURRENT RESEARCH

As discussed above, the use of remote sensing technologies provides several advantages over in-situ observations in heat island analyses. Consequently, existing research has utilized surface temperature as a substitute for air temperature when evaluating the relationship between heat and human health. The main limitation of this approach, however, is that surface temperature is an imprecise indicator of the commonly-used skin temperature relied upon by public health officials. While moderate agreement exists between surface and near-surface air temperature measurements over larger extents [51], this

generalization likely becomes less true with increasing scale. In actuality, the precise relationship at a given location is contingent upon complex physical and atmospheric processes such as advection, for example, which itself is dependent upon the morphology of the built environment [68]. Furthermore, "remote measurements are more sensitive to energy stored in the atmosphere and better representations of large scale climate changes due to greenhouse gas warming and atmospheric circulation, but less sensitive to localized changes happening at the surface such as land cover conversions" [66, p. 32]. Use of near-surface air temperature is therefore more desirable for assessments of the heat-health relationship conducted at higher spatial resolutions.

In Sections 2.3.1 and 2.3.2, the different characteristics that comprise heat vulnerability are identified. While several of the studies referenced above consider the spatial patterns and distributions of either sociodemographic or environmental vulnerability across the urban landscape, most do not examine the spatial coincidence of and interactions between these different vulnerabilities jointly. Of the studies that do assess comprehensive heat vulnerability [48, 28, 63, 56], only one was found that explicitly measured both the spatial clustering of the distinct vulnerabilities as well as cumulative vulnerability to heat [66]. This work builds on that research by measuring the spatial clusters of sociodemographic, environmental, and comprehensive heat vulnerability at a finer scale to better inform mitigation strategies.

In short, of the few studies that use land surface temperature to estimate continuous air temperature, none explore the spatial correlation of air temperature and vulnerability to heat; of the studies that explore the spatial correlation of comprehensive heat vulnerability and temperature, none do so using continuous air temperature estimates. This thesis attempts to bridge the gap between these two arenas by measuring the co-location of elevated air temperatures and comprehensive vulnerability to heat. Furthermore, this work introduces an explicit spatial component into the analysis in an effort to more thoroughly describe the urban heat island phenomenon in relation to the heat vulnerability of urban populations.

CHAPTER III

RESEARCH DESIGN

The primary objective of this research is to analyze the spatial relationship between urban hot spots and populations most vulnerable to heat; this chapter details the overall design and organization of that analysis. What follows herein is a discussion of the research question, criteria used for site selection, data sources employed, and a detailed methodology.

3.1 RESEARCH QUESTION

As a component of both the causes and effects of climate change, cities have a responsibility to confront the public health consequences borne from a warmer future. With limited resources available to municipalities, the most successful mitigation policies will be those designed with respect to both the social and physical environments. Targeting these strategies—spatially or otherwise—necessarily requires a knowledge of both the hottest spaces in the city and the clusters of populations at risk from elevated temperatures. An understanding of where these conditions exist therefore becomes invaluable to policy makers, public health officials, and city planners alike.

This thesis aims to advance current understanding of the relationship between these two spatial processes by answering the following question:

> *Are local hot spots within urban heat islands spatially correlated with populations most vulnerable to extreme heat?*

To do so, it is necessary to identify both the warmest temperatures within the city as well as the clusters of socio-demographically- and environmentally-vulnerable populations.

The central inquiry presented has been developed from a general hypothesis that, in spaces where populations least able to withstand the negative health effects of extreme heat are located, the characteristics of the built environment tend to raise temperatures and exacerbate exposure to heat. Further underlying this analysis is the belief that a positive relationship exists between the different types of vulnerability discussed in Chapter II. It is expected, then, that the results of this work will illustrate a spatial correlation between the two phenomena; that local hot spots will, in fact, be co-located with populations most vulnerable to extreme heat.

3.2 STUDY LOCATIONS

To assess this correlation, the cities of Atlanta, Georgia and Minneapolis, Minnesota were selected due to several key similarities and differences. It is important to note that only the central cities of Atlanta and Minneapolis, defined by the administrative boundary, were

included in this analysis (Figure 5). The decision to exclude the greater metropolitan regions was a result of the relatively uniform land cover and overall population dispersion characteristic of suburban development. Using only the urban core in this study ensures a wide range of land uses and densities, as well as spatially concentrated, yet diverse, populations.

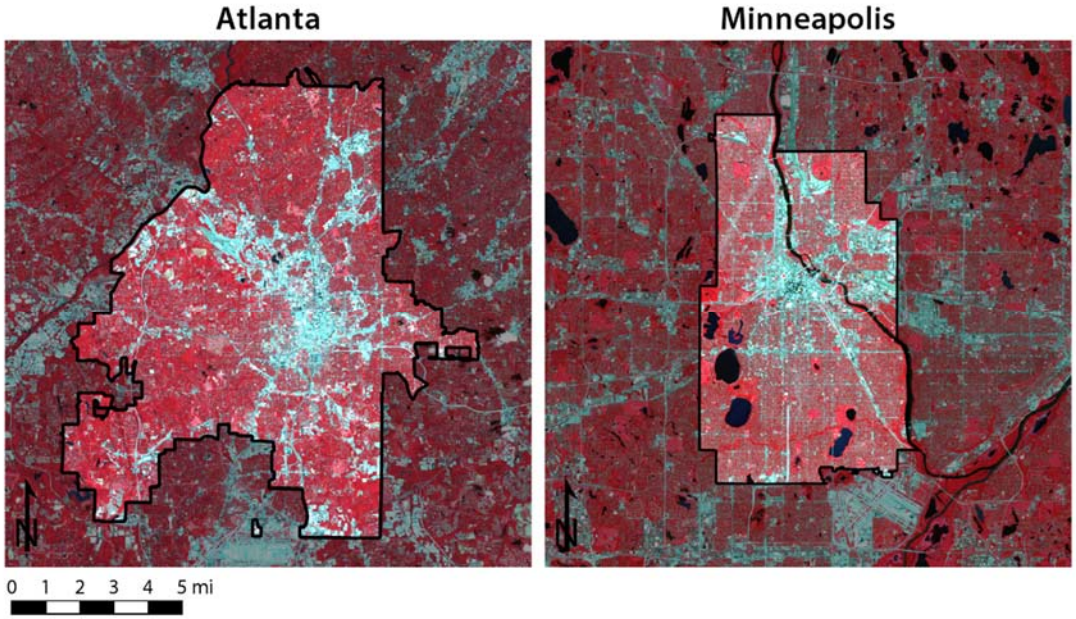

Left: City of Atlanta false-color infrared Landsat TM image acquired on July 30, 2011; Right: City of Minneapolis false-color infrared Landsat image acquired on July 25, 2010. The cities are shown at the same scale.

Figure 5: Cities of Atlanta and Minneapolis

First and foremost, both cities have similarly-sized populations yet exceedingly different population densities (Table 1). As of 2012, the population of Atlanta was an estimated 443,775 with a population density of 3,188 people per square mile; Minneapolis, on the

other hand, had an estimated population of 392,880 and a population density of 7,020 people per square mile—more than double that of Atlanta. This has important implications for urban form and, thus, heat island formation and intensity.

Table 1: Comparison of the Cities of Atlanta and Minneapolis

	Atlanta	**Minneapolis**
Total Population	443,775	392,880
Total Area (mi.^{2})	132.4	58.4
Population Density	3,188	7,020
Average Temperature (°F)	53.2 – 71.9	37.2 – 55.2

Second, these cities were chosen due to the absence of a proximate water body. Because large bodies of water exhibit a moderating influence on temperature and can also alter the moisture characteristics of an area, this selection criteria was vital. Finally, Atlanta and Minneapolis were selected due to their locations in very different climatic regions of the country. While not explicitly accounted for in this analysis, the acclimation of populations in these different regions has meaningful ramifications as the climate continues to warm, and is a significant factor to consider when making policy recommendations to decrease vulnerability.

3.3 DATA

3.3.1 Air and Surface Temperature

The remotely-sensed data used in this analysis were acquired by the Thematic Mapper (TM) sensor on board the Landsat 5 satellite, jointly operated by the United States Geological Survey (USGS) and the National Aeronautics and Space Administration (NASA). The terrain-corrected (level 1T) satellite scenes collected over Minneapolis on July 25, 2010 at 11:48 a.m. and Atlanta on July 30, 2011 at 12:03 p.m., both with less than 10% cloud cover, were downloaded from the USGS Earth Explorer internet platform. Six of the seven spectral bands within the Landsat 5 system—blue, green, red, two mid-infrared, and near-infrared—were acquired at a resolution of thirty meters, while data in the thermal infrared band were originally acquired at a 120 meter resolution, but were resampled to a resolution of thirty meters by NASA prior to download.

Landsat data were selected over other remote sensing products identified in the urban heat island literature because of the comparatively high spatial resolution and temporal consistency of the Landsat satellite. Other options for this analysis included data from the Moderate Resolution Imaging Spectroradiometer (MODIS), on board NASA's Aqua and Terra satellites, and the Advanced Spaceborne Thermal Emission and Reflection Radiometer (ASTER), on board NASA's Terra satellite. MODIS data are perhaps the most widely cited in heat island literature; this is likely due, at least in part, to the availability of both daytime

and nighttime satellite images. However, while MODIS images may be preprocessed for land surface temperature before user acquisition, a spatial resolution of one kilometer made this an unsuitable data source for identifying hot spots on a suburban scale. ASTER data have a spatial resolution of fifteen meters in the very-near infrared, thirty meters in the shortwave infrared, and ninety meters in the thermal infrared; however, data acquisition is not consistent and must be requested and scheduled through NASA.

In addition, date- and time-relevant in-situ observations of air temperature and relative humidity were acquired from two sources: the Quality Controlled Local Climate Dataset from the National Oceanic and Atmospheric Administration (NOAA) National Climatic Data Center, as well as Weather Underground's cooperative network of Personal Weather Stations (PWS). The PWS data, obtained through an application programming interface, were quality-controlled by Weather Underground personnel before being included on the website. Aside from one observation in Atlanta that measured temperatures in excess of 20°F over all other measurements and was removed, these observations were in very close agreement with those recorded by nearby NOAA stations, and were therefore deemed acceptable for use in this analysis (Figure 6).

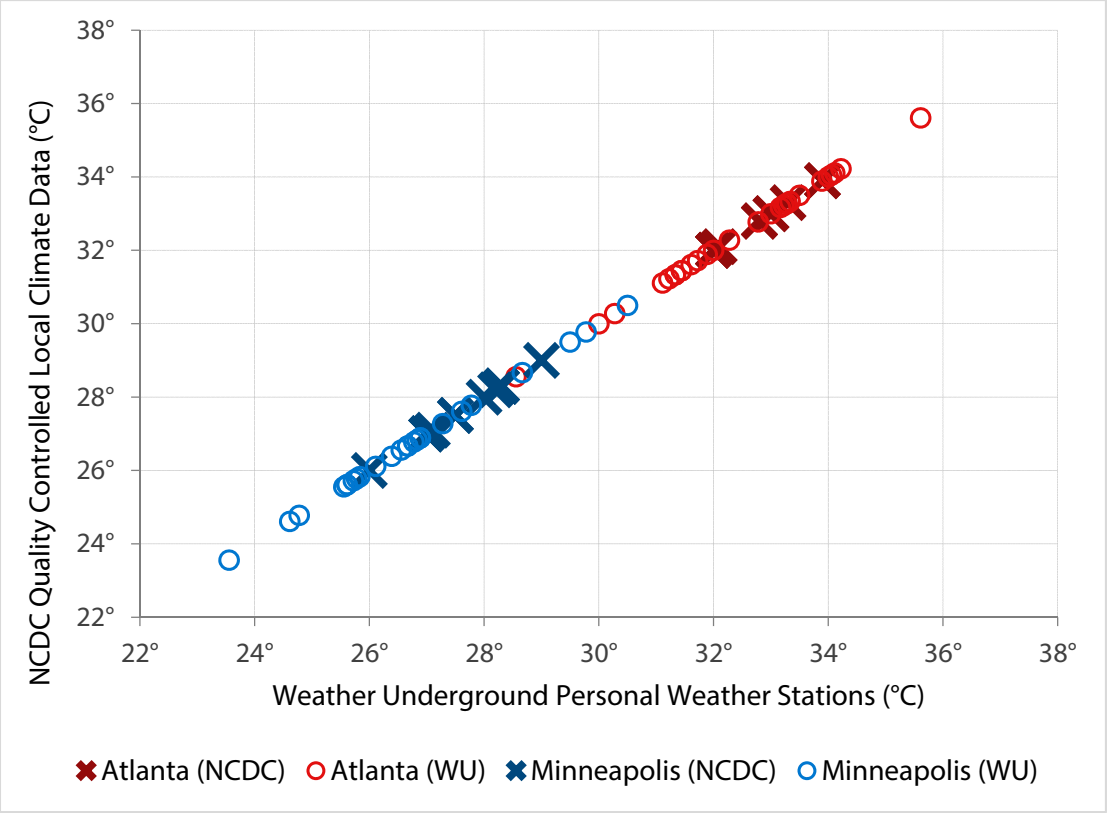

Figure 6: Correlation between NCDC and Weather Underground Stations

3.3.2 Heat Vulnerability

Socioeconomic and demographic data for the cities of Atlanta and Minneapolis were obtained from the United States Census Bureau American Community Survey (ACS) Five-Year Estimates for the years 2008–2012. Specifically, data describing total population, age, race, income, education, household type, and English language proficiency were acquired at the block group level according to the Census Bureau's Topologically Integrated Geographic Encoding and Referencing (TIGER) boundary files. The ACS, an annual statistical survey of 1% of the population, provides continuous demographic, economic, housing, and

social data similar to what was previously available through the Census long form. The five-year estimates used in this work combine the five most recent one-year estimates in order to release data at the block group level while maintaining citizens' overall privacy.

Additionally, land cover data for percentage impervious and percentage tree canopy were obtained from the USGS Land Cover Institute for the years 2006 and 2001, respectively. These datasets, although perhaps somewhat dated at the time of this analysis, offer consistent methodology and results, and provide comprehensive coverage of both study areas. For elevation, thirty meter digital elevation model raster surfaces were obtained from the USGS National Elevation Dataset through the United States Department of Agriculture Natural Resources Conservation Service.

3.4 METHODOLOGY

A three-part methodology was employed to evaluate whether vulnerable populations are co-located with local hot spots in urban heat islands: first, continuous air temperature was estimated from satellite imagery, weather station ground observations, and other variables describing the physical and built environments; second, principal components analysis was performed to generate a heat vulnerability index based on sociodemographic and environmental variables; and third, a statistical analysis was performed to measure the correlation between the hottest air temperatures and the populations most susceptible to the health consequences of extreme heat.

3.4.1 Air Temperature

3.4.1.1 Land Surface Temperature

In order to estimate continuous air temperature and identify suburban hot spots, it was first necessary to derive land surface temperature from the Landsat satellite imagery. This process entailed three primary steps: 1) calculation of top of atmosphere, or at-sensor, brightness temperature; 2) estimation of ground surface emissivity; and 3) application of the mono window algorithm for land surface temperature retrieval. The mono window algorithm used in this study was developed by Qin et al. (2001), and was selected over other methods of surface temperature estimation—such as the temperature-emissivity separation algorithm or the split-channel method—due to its relatively negligible input data requirements [46]. Figure 7 shows the model built to derive land surface temperature using ERDAS Imagine's Model Maker.

3.4.1.1.1 Brightness Temperature

For each scene, the brightness temperature was calculated on a pixel-by-pixel basis using the thermal infrared band exclusively. The procedure employed here was two-tiered—the digital number of each pixel was first converted into spectral radiance, which was then converted into top of atmosphere brightness temperature. A detailed discussion of this process follows in Sections 3.4.1.1.1.1 and 3.4.1.1.1.2.

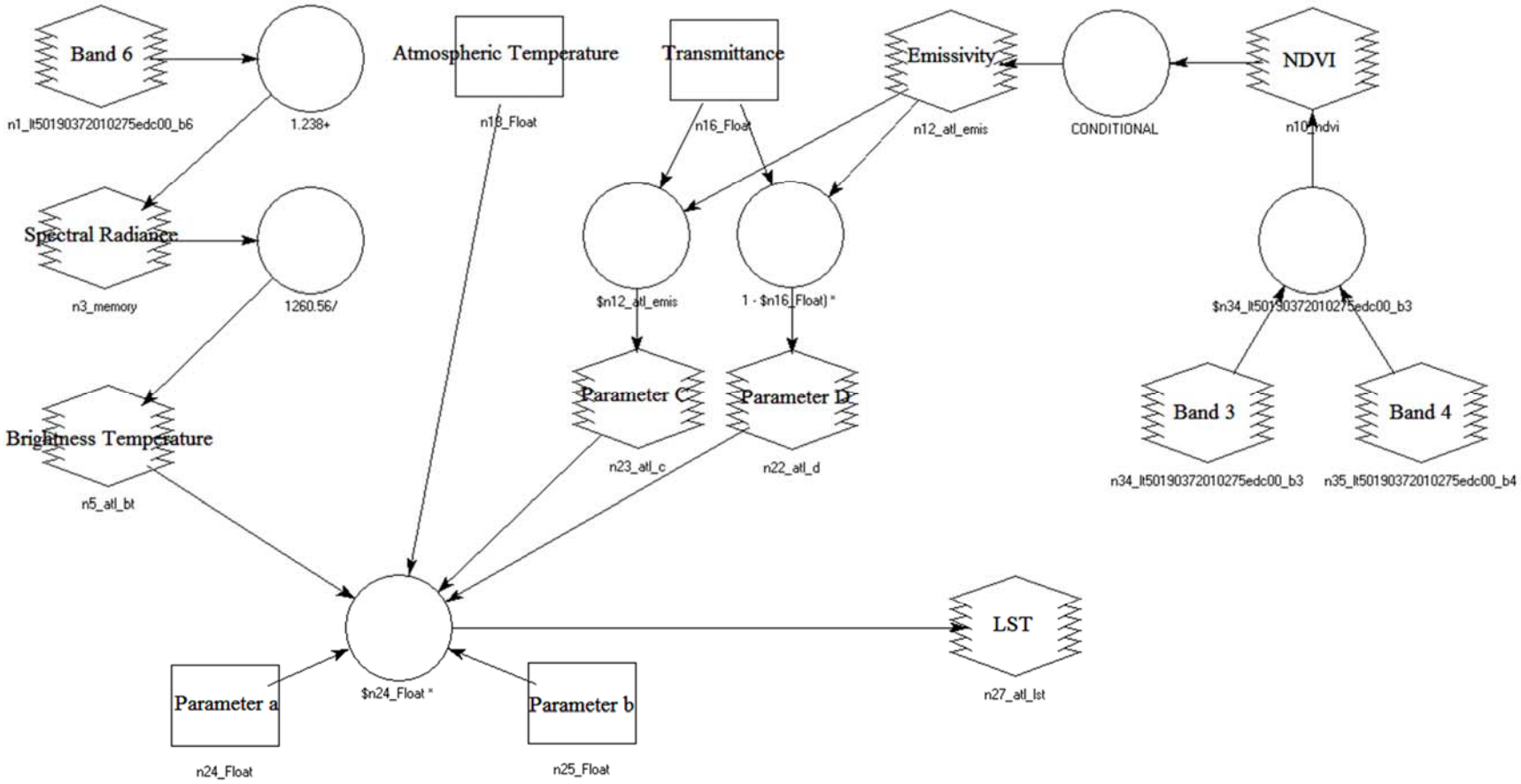

This figure shows the model used to derive land surface temperature from 7 bands of a Landsat TM image, correcting for atmospheric transmittance and emissivity effects.

Figure 7: Satellite Image Processing Model

3.4.1.1.1.1 Spectral Radiance

Landsat TM Band 6 senses radiation in the thermal infrared section of the electromagnetic spectrum—that is, radiation with wavelengths between 10.40 μm and 12.50 μm. The digital number, or radiometric value, of each pixel must be processed in order to obtain an accurate measure of radiation intensity received at-sensor. Equation 1, originally developed by NASA, was used to correct the data for atmospheric attenuation—absorption of radiation that occurs between the land surface and the satellite sensor—and convert the digital number of each pixel (Q_{DN}) into at-sensor spectral radiance (L_λ):

$$L_\lambda = L_{\min(\lambda)} + \left(L_{\max(\lambda)} - L_{\min(\lambda)}\right)\frac{Q_{DN}}{Q_{\max}} \quad (1)$$

where L_λ is measured in W m^{-2} sr^{-1} μm^{-1}; Q_{max} is equal to the maximum digital number in the scene (255 for 8-bit Landsat data); and $L_{min(\lambda)}$ and $L_{max(\lambda)}$ are the corresponding spectral radiances for the minimum and maximum digital numbers in the scene, respectively, and provided in the scene metadata. Given $L_{min(\lambda)}$ and $L_{max(\lambda)}$, the previous equation can be simplified as Equation 2 for Landsat 5 TM6:

$$L_\lambda = 0.1238 + 0.005632156Q_{DN} \quad (2)$$

3.4.1.1.1.2 Calculation of Brightness Temperature

The spectral radiance value for each pixel was then used to calculate at-sensor brightness temperature using the inverse of Planck's radiance function for temperature. This has been included here in modified form as Equation 3, approximated specifically for Landsat TM6 data:

$$T_6 = \frac{K_2}{\ln\left(1+\frac{K_1}{L_\lambda}\right)} \quad (3)$$

where T_6 is the at-sensor brightness temperature in Kelvin; K_1 and K_2 are calibration constants specific to the Landsat TM sensor and provided in the metadata by the satellite manufacturer; and L_λ is the spectral radiance calculated in the previous step using Equation 1.

3.4.1.1.2 Emissivity

Importantly, T_6 is not an actual measure of surface temperatures in the scene, but rather an estimate of land surface temperature if Earth were to emit radiation as a perfect blackbody. Because of this, the remotely-sensed spectral radiance data values must be corrected for the emissive properties of Earth's surfaces. In this analysis, the ground surface emissivity of each pixel was estimated from normalized difference vegetation index (NDVI).

3.4.1.1.2.1 Calculation of NDVI and Ground Surface Emissivity

NDVI, a common measure of the amount of healthy vegetation in a scene, is calculated using the near infrared (ρ_4) and visible red (ρ_3) bands due to the high reflectivity of chlorophyll in the infrared section of the electromagnetic spectrum. NDVI was calculated for both Atlanta and Minneapolis using Equation 4:

$$\mathrm{NDVI} = \frac{(\rho_4 - \rho_3)}{(\rho_4 + \rho_3)} \tag{4}$$

This resulted in an index of floating point values ranging from 1 to 1, with areas of open water approaching 1, areas of bare ground near 0, and areas of lush vegetation approaching 1. Using these NDVI values, Van De Griend and Owe (1993) first proposed Equation 5 to estimate surface emissivity, specifically for NDVI values ranging from 0.157 to 0.727 [65].

$$\varepsilon = 1.0094 + 0.0047 \ln(\mathrm{NDVI}) \tag{5}$$

A more comprehensive method for estimating surface emissivity for all NDVI values, presented by Zhang et al. (2006), was used in this analysis (Table 2) [70].

Table 2: Estimated Ground Surface Emissivity by NDVI Range

NDVI	Emissivity (ε)
NDVI < -0.185	0.995
-0.185 ≤ NDVI < 0.157	0.970
0.157 ≤ NDVI ≤ 0.727	$1.0094 + 0.0047 \times \ln(NDVI)$
0.727 < NDVI	0.990

Here, an emissivity value of 0.995 is assigned to areas presumed to be covered in water; a value of 0.970 is assigned to areas presumed to be covered in materials used in construction of the built environment (asphalt or concrete, for example) with higher relative thermal capacities; a value of 0.990 is assigned to areas covered in dense, healthy vegetation; and Equation 5 is used to calculate the emissivity value for all other areas.

3.4.1.1.3 Calculation of Mean Atmospheric Temperature

The final two input parameters used in the mono window algorithm require supplemental in-situ data observations. For each Landsat scene, average near-surface air temperature and relative humidity were calculated using the location and time-relevant NCDC and Weather Underground observations. Given the location of both cities and the date both satellite images were acquired, a mid-latitude summer atmospheric model was used to determine mean atmospheric temperature. Assuming a clear, cloud-free sky and little to no

vertical turbulence, effective mean atmospheric temperature is a linear function of near-surface air temperature (Equation 6):

$$T_a = 16.0110 + 0.92621 \times T_0 \quad (6)$$

where T_a is mean atmospheric temperature and T_0 is average near-surface air temperature, both measured in Kelvin.

3.4.1.1.4 Estimation of Atmospheric Transmittance

Through sensitivity analysis, Qin et al. (2001) determined that atmospheric transmittance is the most important input parameter in the mono window algorithm [46]. The precise value of transmittance in a scene is generally calculated with complex atmospheric modeling programs such as LOWTRAN or MODTRAN; however, this can also be estimated using the water vapor content present on the date and time of satellite overpass. Equation 7 was used to calculate water vapor content using in-situ temperature and relative humidity observations.

$$w_i = 0.0981\left\{6.108e^{\left[\frac{17.72\times(T_0-273.15)}{237.3+(T_0-273.15)}\right]} \times RH\right\} + 0.1697 \quad (7)$$

where w_i is water vapor content (g/cm^2), T_0 is near-surface air temperature (K), and RH is relative humidity. Using this estimate of water vapor content and the mean atmospheric

temperature from Equation 6, atmospheric transmittance was then calculated for each scene using Equation 8:

$$\tau_i = 1.031412 - 0.11536 \times w_i \quad (8)$$

where τ_i is transmittance and w_i is water vapor content (g/cm^2).

3.4.1.1.5 Land Surface Temperature Retrieval

The following algorithm was used to derive land surface temperature (Equation 9):

$$T_s = \frac{\{a(1-C-D)+[b(1-C-D)+C+D]T_6-(D\times T_a)\}}{C} \quad (9)$$

where:

$$a = 67.355351$$
$$b = 0.458606$$
$$C = \varepsilon_i \times \tau_i$$
$$D = (1 - \tau_i)[1 + (1 - \varepsilon_i) \times \tau_i]$$

Here, T_s is final land surface temperature (K); T_a is mean atmospheric temperature (K); T_6 is brightness temperature (K); ε_i is emissivity; τ_i is atmospheric transmittance; and *a* and *b* are constants specific to Landsat 5 provided by the satellite manufacturer.

3.4.1.2 Spatial Regression

To accurately estimate air temperature continuously across the study areas, it was necessary to assess how well the independent variables explained variance in air temperature at the locations for which observations were recorded. Using the averages of land surface temperature, NDVI, emissivity, elevation, and latitude within a one kilometer buffer around each observation as independent variables, a single regression model was developed to better understand both the relationship of the independent variables to air temperature and also their ability to predict the air temperature in locations where a direct observation did not exist. All spatial regression functions were carried out using GeoDa 1.4.6 software.

Regression is a statistical tool used to predict or explain values of a dependent variable given one or more independent variables. Arguably the most common example employed in city planning, ordinary least squares (OLS) regression models approximate a linear relationship between the dependent variable and one or more independent variables by minimizing the sum of the squared error terms. To generate meaningful inferences from OLS, several assumptions must be made regarding the data underlying the regression model: 1) that the error terms are normally distributed; 2) that the errors have a constant variance; 3) that the observations are independent; 4) that the relationship between the dependent and independent variables is linear; 5) that the error term is independent over time; and 6) that all relevant independent variables have been included. In spatial analysis, however, it is well-

understood that proximate observations often exhibit spatial dependence and thus violate several of these aforementioned assumptions; in fact, multiple regression assumptions are in direct contrast with Tobler's first law of geography, which states that "everything is related to everything else, but near things are more related than distant things" [62, p. 3]. Regression models that do not account for this spatial dependence, such as OLS, introduce biases that ultimately increase the chances of a Type I error.

To more accurately model the relationship between the predictive variables and air temperature, it was first necessary to estimate a simple OLS model (Equation 10):

$$y_i = a + \beta_1 x_1 + \beta_2 x_2 + \beta_3 x_3 + \beta_4 x_4 + \beta_5 x_5 + \varepsilon \quad (10)$$

where y_i is observed air temperature (°C); *a* is the intercept of the regression line; β_n are regression parameters; x_1 is latitude (geographic degrees north); x_2 is NDVI; x_3 is emissivity; x_4 is elevation (m); x_5 is land surface temperature (K); and ε is the error term.

Global Moran's I, or the degree to which similar features tend to be clustered together, was then calculated to quantify the spatial autocorrelation among the OLS residual terms; this was found to be significant at 99.99%. In order to reduce this autocorrelation, a spatial autoregressive model was specified for this work. Also known as a spatial lag model, this type of regression is used explore spatial processes where the value of the dependent variable, y, in any given location is influenced by the values of y in adjacent locations. This spatial

dependence was built into the model with the inclusion of a spatially-lagged version of air temperature as an independent variable, capable of affecting the value of the (unlagged) dependent air temperature variable (Equation 11):

$$T_{air} = a + \rho W(T_{air}) + \beta_1(latitude) + \beta_2(NDVI) + \beta_3(emissivity) + \beta_4(elevation) + \beta_5(land\ surface\ temperature) + \varepsilon \quad (11)$$

where ρ is the autoregressive parameter of T_{air}; and W_{Tair} is the spatial lag of T_{air} given the weights matrix W.

A Euclidean threshold distance of 500 meters was used to create the spatial weights matrix for this analysis. Use of this distance weight dictates that values within a circle with a radius equal to 500 meters from a given measurement location assert influence on the value at that location. This is appropriate for explaining variance in air temperature, which is generally a smooth function with gradual changes occurring over larger areas.

3.4.1.3 Geostatistical Interpolation

The final step in determining the location of urban hot spots was to estimate a continuous layer of air temperature. The approximation of values over locations that did not have a temperature measurement was accomplished using the observed air temperature values, the variables found to be statistically significant in the spatial lag regression (Section 3.4.1.2), and a geostatistical interpolation method known as cokriging. According to

Bohling (2005), kriging is defined as "optimal interpolation based on [linear] regression against observed z values of surrounding data points, weighted according to spatial covariance values" [5]. Cokriging, then, is a distinct method of kriging that utilizes the autocorrelation and spatial cross-covariance between multiple correlated variables to reduce the variance of the estimation error. Specifically, ordinary cokriging was used herein because of its applicability to the interpolation of a continuous raster surface from multivariate data, and due to its assumption of locally-constant, rather than globally-constant, mean values. The geostatistical interpolation, and semi and covariogram estimation functions were conducted using ArcGIS 10.1 software.

3.4.2 Heat Vulnerability Index

Another focus of this thesis is on generating a heat vulnerability index at the block group level, which will allow greater spatial specificity of adaptive mitigation policies. To achieve this, the general methodology of Reid et al. (2009) was employed with only slight modifications, similar to Vargo (2012). Principal components analysis was performed on variables for total population, age, race, income, education, language proficiency, household type, and land cover at the block group level. To facilitate interpretation of the results, the factor scores were normalized around a mean of zero and reclassified based on standard deviation from the mean; the final vulnerability index is a linear combination of those reclassified factors. The variables chosen to indicate different heat vulnerabilities, as well as

the statistical and spatial analysis methods used to generate a comprehensive heat vulnerability index, are discussed in the following sections.

3.4.2.1 Vulnerability Variables

3.4.2.1.1 Sociodemographic Vulnerability

The variables that comprise sociodemographic vulnerability include total population; individuals over age 65; individuals identified as nonwhite; households with an annual income of less than $20,000; individuals with less than a high school diploma; individuals who spoke English 'not well' or 'not at all'; individuals living alone; and individuals over 65 and living alone.

Together, the English language proficiency and household type variables were used as a proxy to account for increased vulnerability from social isolation as described in Chapter II. As previously discussed, individuals who are linguistically isolated and those who lack a strong, connected social network are less likely to seek assistance and therefore more vulnerable to the threat of heat.

The variables above were calculated as a percentage for each block group for several reasons. First, this decision was made to account for overall population distribution with each city. If the raw values were used, each variable would likely mimic the distribution of

population itself instead of highlighting certain areas with more densely clustered vulnerabilities. Second, the use of percentages attempts to account for the area of each Census block group. Because the block group is based on population and is not areally-consistent—it is not always one square mile or four city blocks, for example—it is necessary to consider the heterogeneity of spatial units when comparing between entities.

3.4.2.1.2 Environmental Vulnerability

The land cover variables used to estimate vulnerability were generated by recoding the land cover types present in the Atlanta and Minneapolis areas into six general classes, of which two—vegetation and urban—were extracted for use in this analysis. Similar to the sociodemographic vulnerability variables, each recoded land cover class was then computed as a percentage by block group. The original land cover types and recoded values are shown in Table 3.

Table 3: Scheme for Recoding Land Cover Classes

Original Land Cover	Recoded Land Cover
Open water	Water
Woody wetlands; Emergent herbaceous wetlands	Wetland
Developed, open space; Shrub/scrub; Grassland/herbaceous; Pasture/hay; Cultivated crops	Grass/Shrub
Deciduous forest; Evergreen forest; Mixed forest	Vegetation
Developed, low intensity; Developed, medium intensity; Developed, high intensity	Urban
Barren land	Barren

For both Atlanta and Minneapolis, the vegetated class included scrub/shrub, palustrine forested wetland, cultivated crops, pasture/hay, grassland/herbaceous, deciduous forest, evergreen forest, and mixed forest land cover; while the urban class included high, medium, and low intensity developed land cover. The land cover reclassification was performed using ERDAS Imagine software.

3.4.2.1.3 Relationships among Vulnerability Elements

To investigate the nature of the relationships between vulnerability elements more thoroughly, Pearson's product-moment correlation coefficient (r) was calculated for each

pair of variables for each city. Pearson's r facilitated an improved understanding of the structural complexity underlying vulnerability to heat, and, along with the results of subsequent spatial analyses, may be used to help create customized strategies for addressing vulnerability to heat.

3.4.2.2 Principal Components Analysis

Principal components analysis (PCA) is a statistical function used to simplify data by reducing its dimensionality. To deconstruct multi- or hyper-variate data, PCA transforms a matrix with m observations and n variables ($m \times n$) into a matrix with m observations and f new and independent components ($m \times f$ where $n \geq f$). The principal component (that with the highest eigenvalue) explains the maximum variance in the data, with each successive component explaining the most variance remaining unaccounted for. Conceptually, this can be understood as 'projecting' the data in a mathematical space. For example, during PCA, data on an x,y plane is reprojected onto a new dimension where the planar axes f_1 and f_2, representing the eigenvectors of the data, are positioned orthogonally such that their directions create the most variance within the data points.

In this analysis, PCA was performed using a direct Oblimin rotation to allow for correlation among the factors. Based on the conventional criteria of having eigenvalues greater than one as well as interpretation of the scree test, four components were selected for both Atlanta and Minneapolis. Following Reid et al. (2009), factor scores for each block group

for each component were normalized around a mean of zero and a standard deviation of one [48]. To build a vulnerability index, these component scores were then reclassified as integers based on distance from the mean.

Component scores more than two standard deviations below the mean received a value of 1, indicating lowest vulnerability to heat; component scores between one and two standard deviations below the mean received a value of 2; component scores between the zero and one standard deviation below the mean received a value of 3; component scores between the zero and one standard deviation above the mean received a value of 4; component scores between one and two standard deviations above the mean received a value of 5; and component scores more than two standard deviations above the mean received a value of 6, indicating highest vulnerability to heat. When necessary, the calculated component scores were inverted to ensure directional agreement between increased vulnerability and larger reclassified values. As the relative influence of each component on heat risk is unknown, the reclassified values were each given equal weight and summed to create the final heat vulnerability index.

3.4.2.3 Spatial Autocorrelation of Vulnerabilities

Local Moran's I, or Local Indicators of Spatial Autocorrelation (LISA), was used to identify the statistically significant block group clusters and outliers for each of the principal

components, as well as for the linear combination of the components representing comprehensive vulnerability. Whereas global Moran's I is a measure of spatial autocorrelation in an entire dataset, LISA shows—for each feature—global-local degrees of autocorrelation that are statistically significant based on the neighboring features of each entity. Put simply, while global Moran's I answers the question of whether or not an overall spatial pattern exists, LISA specifies where the pattern exists. This information can help city planners, public health officials, and policymakers identify which strategies to reduce different types of vulnerability are most appropriate in each area.

The linear combination of the principal components was used to determine significant clusters and outliers of comprehensive heat vulnerability over the sum of the recoded components for two reasons: first, it is necessarily a more precise measure, as the recode function assigned a short integer value to observation groups based on distance from the mean, and the original summed components scores were floating point numbers; and second, a reclassification was performed simply to facilitate interpretation of relative vulnerability in each city, and because LISA determines spatial autocorrelation—the correlation of a feature with itself—no complex explanation is necessary. Computing LISA using the sum of the principal components was also beneficial insofar as it indicated areas in which highly vulnerable populations are clustered together at a more precise resolution.

In this analysis, neighboring features were distinguished using a row-standardized first order queen contiguity spatial weights matrix, which defines the neighbors of each input observation as those which have a shared corner or edge with that observation.

3.4.3 Spatial Correlation of Temperature and Vulnerability

The final step in this analysis involved establishing the degree to which the hottest air temperatures and most vulnerable populations were spatially correlated. This was measured using a version of Local Moran's I modified for use in bivariate analyses.

3.4.3.1 Grid Overlay

In order to calculate spatial correlation between two variables, the data must be of the same architecture: both in continuous raster format or both in discrete vector format. Because these two data formats are implicitly dissimilar, the spatial statistical methods that may be applied differ substantially for each. A common approach to this challenge is data conversion, whereby the data are transformed into a single format.

To ensure spatial interoperability, and because of the complex nature of geostatistical correlation analysis of continuous variables, air temperature was converted into a vector format. First, a 500 meter fishnet grid was generated over each city. Using the Zonal Statistics tools provided in ArcGIS, mean air temperature was calculated for each grid cell; Geoprocessing tools were used to calculate the mean heat vulnerability index score for each cell

as well. This process resulted in a grid of 500 meter cells covering each city, where each cell contained average air temperature and heat vulnerability index values. With both air temperature and vulnerability data in discrete vector format, several spatial statistical methods to evaluate correlation were applicable. This analysis utilizes Bivariate Local Moran's I.

3.4.3.2 Bivariate Local Moran's I

The final step in the statistical analysis employed Bivariate Local Moran's I to discern the extent to which the hottest air temperatures and the populations most vulnerable to heat are spatially correlated. Similar to the LISA statistic used above to assess degrees of global-local spatial autocorrelation in each of the principal components, Bivariate LISA can be used to evaluate the nature and strength of spatial correlation between two variables. In this analysis, Bivariate LISA measured the correlation between heat vulnerability in each cell and air temperature values in the neighboring grid cells using a first order queen contiguity spatial weights matrix.

CHAPTER IV

RESULTS

This chapter presents the results of the analysis conducted to evaluate the co-location of hot spots and vulnerable populations across the urban environment. The chapter begins with an examination of the approximated continuous air temperature layer, with a discussion of potential sources of error and uncertainty introduced throughout the estimation process. Following, a detailed summary of the principal components analysis and subsequent comprehensive heat vulnerability index. The chapter concludes with an overview of the computed spatial correlation between the hottest local temperatures and the most vulnerable populations in each city.

4.1 AIR TEMPERATURE

Following the methodology presented in Chapter III, air temperature was estimated from land surface temperature, NDVI, emissivity, elevation, and latitude data using a spatial regression model (Figure 8). In an attempt to control for any potential hyper-local influences on air temperature introduced by the site of each measurement station, average values for the independent variables were calculated within a one kilometer buffer around each observation location. By providing a general summary of the physical properties of an area

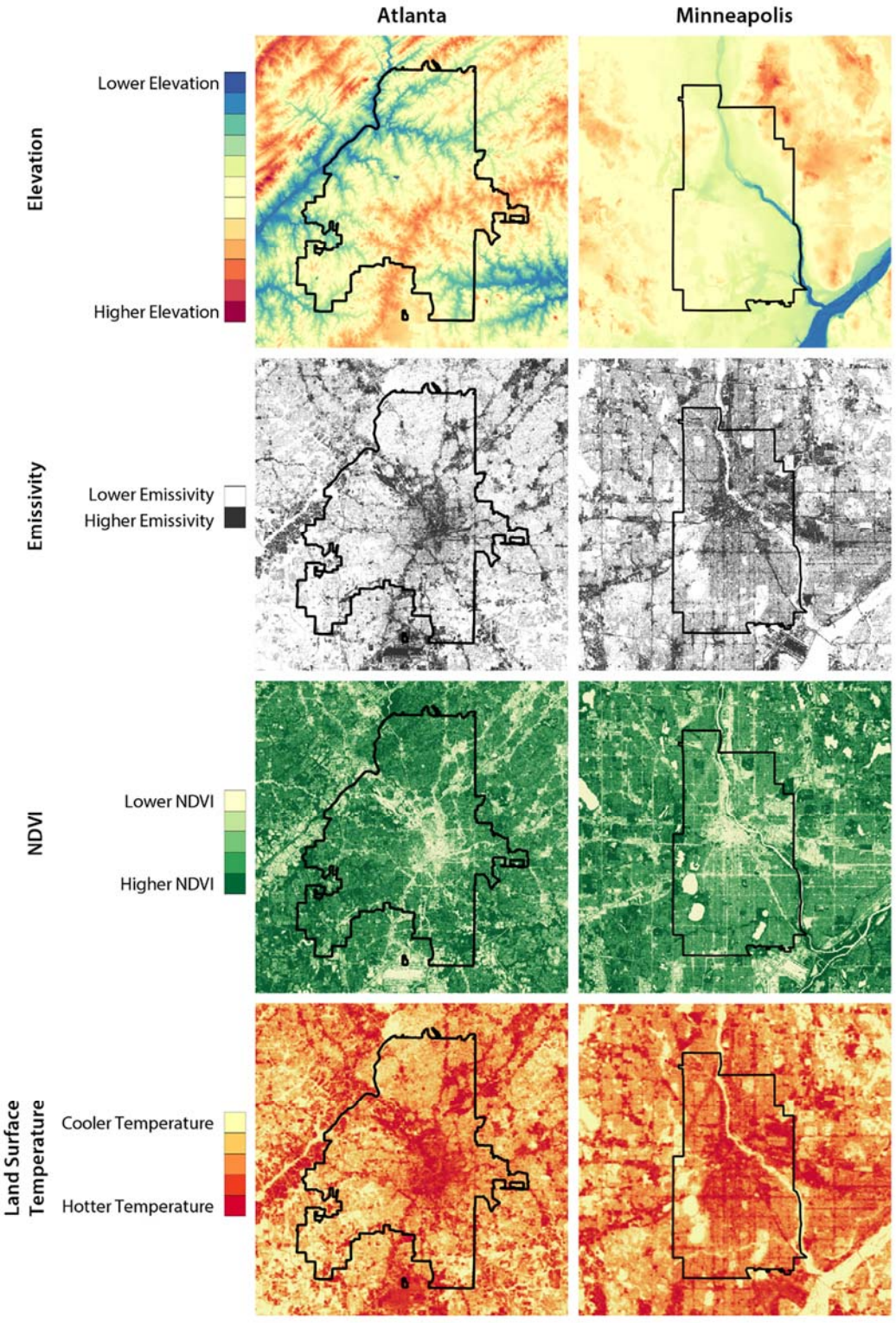

Figure 8: Variables used to Estimate Air Temperature

instead of information about a discrete point, the influence of any site-specific surface anomalies affecting local temperature is substantially reduced.

4.1.1 Spatial Regression

The values of the independent variables were extracted around each of the sixty temperature observation points—thirty of which were located in the Atlanta area and thirty of which were located in the Minneapolis area—to predict air temperature across locations without direct observations. Descriptive statistics of the dependent and independent variables for Atlanta and Minneapolis are presented in Table 4.

Table 4: Descriptive Statistics for Air Temperature Prediction Variables

		Mean	Minimum	Maximum	Standard Deviation
Atlanta	NDVI	0.370	0.018	0.540	0.119
	Emissivity	0.968	0.924	0.980	0.001
	Elevation (m)	288.504	245.398	314.345	20.730
	Land Surface Temperature (K)	307.611	301.969	319.544	3.373
	Air Temperature (°C)	32.572	28.556	35.611	1.478
Minneapolis	NDVI	0.394	0.031	0.680	0.130
	Emissivity	0.972	0.964	0.987	0.005
	Elevation (m)	270.325	211.695	319.848	19.791
	Land Surface Temperature (K)	306.525	299.474	312.908	3.222
	Air Temperature (°C)	27.051	23.556	30.500	1.456

Using a Euclidean threshold distance of 500 meters to generate the spatial weights matrix, the spatial lag regression of air temperature yielded the following results (Equation 12):

$$T_{air} = 194.2147 - 0.0424W(T_{air}) - 0.5351(latitude) - 0.2226(NDVI) - 82.8604(emissivity) - 0.0187(elevation) - 0.1834(land\ surface\ temperature) + \varepsilon \quad (12)$$

Detailed results from the model are shown in Table 5. A statistically significant ($p<0.05$) R-squared value of 0.811788 indicates approximately 81.2% of the variation in air temperature can be explained by the average surrounding air temperature (or spatial lag), as well as the average surface temperature, elevation, NDVI, and latitude values around those locations.

Important to note, however, is the lack of statistical significance ($p<0.1$) for NDVI and land surface temperature; this does not imply that these variables are substantively insignificant—in actuality, they are two of the most commonly cited contributing factors to heat island formation—it simply suggests that their influence on the variation of air temperature values cannot necessarily be distinguished from that which would have occurred by chance. The variables for which the coefficients were statistically significant were retained for use in further analysis.

Table 5: Results of Spatial Regression

R-squared	0.812
Standard Error	1.323
Akaike Info Criterion	234.884

Variable	**Coefficient**	**Standard Error**	**z-value**	**Probability**
Spatial Lag (T_{air})	-0.425	0.190	-0.224	0.093
Constant	194.215	82.702	2.348	0.019
Latitude	-0.535	0.098	-5.480	0.000
NDVI	-0.223	2.245	-0.099	0.921
Emissivity	-82.860	45.647	-1.815	0.069
Elevation	-0.019	0.008	-2.206	0.027
Surface Temperature	-0.183	0.137	-1.338	0.181

4.1.2 Geostatistical Interpolation

Using the ArcGIS Geostatistical Wizard, ordinary cokriging models were generated to estimate continuous air temperature from emissivity, elevation, and latitude data for Atlanta and Minneapolis individually. Informed by a trend analysis plot, second order polynomial trend removal of the dependent variable was conducted for both cities to satisfy the assumption of normality and improve the predictive accuracy of the models. Additionally, the input parameters were optimized for each covariogram by means of cross validation in

order to minimize the root mean squared (RMS) error of the resulting estimates. Table 6 displays the output statistics for the cokriging models developed to predict air temperature for the cities of Atlanta and Minneapolis.

Several of the above values reveal issues with various covariogram estimates and, therefore, the resulting prediction layers. Overall, the statistics command greater concern for the model of Minneapolis, and suggest the model of Atlanta is better fit to the input data.

Table 6: Summary of Co-Kriging Models

	Atlanta	**Minneapolis**
Nugget	1.229; 0.003; 169.693	6.076; 0.009; 17.615
Mean	0.012	0.094
Mean Standardized	0.010	0.050
RMS Error	1.436	2.144
RMS Error Standardized	1.242	1.804
Average Standard Error	1.155	1.547

Nugget values represent latitude, emissivity, and elevation, respectively

A relatively large nugget effect was observed between air temperature and elevation in both cities: in Atlanta, this value was 169.6932; and in Minneapolis, this value was 17.6147. Theoretically, the variance of a model at the origin (h=0) is always equal to 0;

however, as lag distance increases (h>0), the nugget effect represents the initial discontinuity in variance [8]. A large covariogram nugget indicates considerable variation between values at small distances, and may be suggestive of measurement error and/or inadequate sample size.

Though the standardized RMS error values imply slight bias in the prediction errors for both models, mean standardized values near 0 indicate that the model estimates are acceptable for both cities. However, discrepancies between the average standard error and RMS values—larger for Minneapolis than for Atlanta—reveal uncertainty of the predicted values is underestimated. This implies that the modeled prediction standard errors are likely smaller than the true values.

4.1.2.1 Potential Sources of Error

It is important to note several possible sources of error likely influencing the accuracy and validity of these predictive models. Chief among these is sample size. Although no universal threshold for minimum number of observations exists—and any requirements would be case specific, nevertheless—previous work suggests at least 100 observations may be necessary to accurately estimate a variogram [7]. Considering only thirty air temperature observations were available for each city, sample size is perhaps the principal factor limiting the precision of these results. It is plausible, then, that merely increasing sample size would improve the predictive accuracy of the models.

Furthermore, cokriging interpolation requires a relatively regular and consistent arrangement of variable observations across the study area. As both expansive areas lacking proximate observations and dense clusters of measurement points can be identified in each city, the spatial distribution of air temperature locations likely contributed to model imprecision as well.

For the reasons addressed in Section 4.1.2 and directly above, it has been determined that the continuous estimates of air temperature across both Atlanta and Minneapolis are unreasonable; the prediction errors generated from the models exceed that which is considered acceptable for this work. Therefore, land surface temperature will be used in all subsequent analyses.[1] As discussed in Chapter II, moderate agreement exists between surface temperature and near-surface air temperature throughout the urban environment. It is expected, then, that this decision will not significantly alter the overall findings of this study.

[1] Unlike air temperature which is diffusive across space, land surface temperature is distinct to each of the different surfaces in an area. Because of the increased spatial precision afforded by surface temperature measurements, a 120 meter grid will replace the previously specified 500 meter grid in future analysis.

4.2 HEAT VULNERABILITY

4.2.1 Sociodemographic and Environmental Vulnerability

The comprehensive heat vulnerability index generated in this analysis was comprised of eight sociodemographic and two environmental variables. Descriptive statistics of these variables at the block group level for Atlanta and Minneapolis are presented below (Table 7).

Of the two cities, Atlanta exhibited a higher average percentage per block group of all vulnerability variables with the exception of "percent of individuals with limited English proficiency" and "percent of land cover considered urban." The variable displaying the greatest average difference between the two locations was "percent of individuals identified as a race other than White," with a mean value of 61.25% in Atlanta and 30.38% in Minneapolis. The variables "percent of individuals living alone" and "percent of individuals identified as a race other than White" exhibited a large range (greater than 80%) in both cities. Additionally, "percent of individuals over 65 and living alone" and "percent of individuals with limited English proficiency" had relatively small standard deviations (less than 10%) in the cities, illustrating a reduced amount of variation among block groups in both localities.

Table 7: Descriptive Statistics for Vulnerability Variables

		Total Population	Population over 65	Race other than White	Less than HS Diploma	Living Alone	Over 65 & Living Alone	Low Income	Limited English Proficiency	Percent Vegetation	Percent Urban
Atlanta	Mean	1385.31	0.109	0.613	0.091	0.200	0.043	0.120	0.017	-0.394	0.330
	Median	1188.00	0.091	0.700	0.072	0.160	0.028	0.103	0.000	-0.419	0.280
	Minimum	182.00	0.000	0.000	0.000	0.000	0.000	0.000	0.000	-0.746	0.049
	Maximum	8226.00	0.549	1.000	0.416	0.814	0.401	0.751	0.457	-0.008	0.911
	Standard Deviation	838.03	0.087	0.369	0.082	0.138	0.051	0.096	0.047	0.187	0.194
Minneapolis	Mean	1018.58	0.089	0.304	0.075	0.178	0.037	0.096	0.046	-0.105	0.475
	Median	931.00	0.073	0.223	0.049	0.148	0.025	0.070	0.013	-0.091	0.467
	Minimum	347.00	0.000	0.000	0.000	0.000	0.000	0.000	0.000	-0.469	0.105
	Maximum	4513.00	0.821	0.972	0.688	1.000	0.821	1.000	0.596	0.000	0.866
	Standard Deviation	421.71	0.079	0.252	0.083	0.130	0.057	0.099	0.074	0.080	0.133

With the exception of Total Population, all values are given in percent.

4.2.1.1 Relationships among Vulnerability Elements

Of particular interest to this work is the coincidence between sociodemographic and environmental heat vulnerability across the urban environment, as the nature of this correlation may offer insight into which strategies will prove most cost effective and produce the most favorable outcomes if implemented. Pearson's r values for the sociodemographic and environmental heat vulnerability variables are presented in Table 8.

Positive correlation implies strategies to reduce vulnerability in one variable will likely have the added benefit of reducing vulnerability in the other. Negative correlation, on the other hand, implies actions aimed at the abatement of one variable will likely fail to decrease the other. For example, population over 65 exhibited negative correlation with all environmental vulnerability elements in both cities, although the relationship with elevation in Atlanta was not found to be statistically significant. From this information, planners and policymakers may infer that strategies aimed at reducing heat are unlikely to benefit elderly populations in the cities of Atlanta and Minneapolis.

.2.2 Principal Components Analysis

Following the methodology used by Reid et al. (2009), PCA was conducted to reduce the dimensionality of the original vulnerability variables. Four components were selected4 for use in generating the comprehensive heat vulnerability index for each city based on

Table 8: Correlation between Vulnerability Variables

		Total Pop.	Pop. over 65	Race other than White	Less than HS	Living Alone	Over 65 & Living Alone	Low Income	Limited English Proficiency	Vegetation	Urban
Atlanta	Pop. over 65	-0.199		0.110	0.181	0.142	0.790	0.267	-0.079	-0.294	-0.288
	Race other than White	-0.028	0.110		0.647	-0.274	0.034	0.509	-0.041	0.099	-0.019
	Less than HS	-0.171	0.181	0.647		-0.198	0.130	0.482	0.192	0.104	0.015
	Living Alone	-0.120	0.142	-0.274	-0.198		0.424	0.379	0.006	0.442	0.486
	Over 65 & Living Alone	-0.159	0.790	0.034	0.130	0.424		0.426	-0.028	-0.004	-0.003
	Low Income	-0.173	0.267	0.509	0.482	0.379	0.426		0.033	0.329	0.256
	Limited English Proficiency	0.135	-0.079	-0.041	0.192	0.006	-0.028	0.033		0.108	0.110
	Vegetation	0.054	-0.294	0.099	0.104	0.442	-0.004	0.329	0.108		-0.953
	Urban	0.070	-0.288	-0.019	0.015	0.486	-0.003	0.256	0.110	-0.953	
	Elevation	-0.147	-0.055	0.162	0.147	0.172	0.069	0.224	-0.132	0.431	0.437
Minneapolis	Pop. over 65	-0.147		-0.090	0.128	0.334	0.778	0.270	0.064	-0.085	-0.123
	Race other than White	0.124	-0.090		0.618	-0.094	0.089	0.434	0.430	0.257	0.270
	Less than HS	0.106	0.128	0.618		0.104	0.345	0.567	0.793	0.315	0.362
	Living Alone	-0.074	0.334	-0.094	0.104		0.559	0.620	0.043	0.329	0.357
	Over 65 & Living Alone	-0.130	0.778	0.089	0.345	0.559		0.588	0.279	0.076	0.079
	Low Income	0.080	0.270	0.434	0.567	0.620	0.588		0.430	0.405	0.474
	Limited English Proficiency	0.145	0.064	0.430	0.793	0.043	0.279	0.430		0.256	0.299
	Vegetation	0.187	-0.085	0.257	0.315	0.329	0.076	0.405	0.256		-0.785
	Urban	0.209	-0.123	0.270	0.362	0.357	0.079	0.474	0.299	-0.785	
	Elevation	-0.131	-0.091	0.072	-0.011	-0.122	-0.112	-0.166	-0.016	-0.229	-0.149

Statistically significant relationships are shown in black

their eigenvalues and interpretation of the scree test. In both Atlanta and Minneapolis, the four retained components cumulatively explained approximately 80% of the variance in the original data. The rotated factor loadings and percentage of variance explained by each component are presented in Table 9.

For each component, variables with values greater than |0.4| were considered to show significant loading. Components were then interpreted as indicating a type of vulnerability based on the variables for which factor loadings were significant. In Atlanta, the first and

Table 9: Results of Principal Components Analysis

	Atlanta				Minneapolis			
	1	2	3	4	1	2	3	4
Total Population	.731	.121	-.240	.364	.603	-.111	.328	.588
Population over 65	.652	-.504	.422	-.147	.477	.694	-.125	-.120
Race other than White	.774	.015	-.474	-.150	.708	-.461	.319	-.075
Less than HS Diploma	.604	.058	-.513	-.332	.785	-.314	.182	-.303
Living Alone	.516	.421	.491	.372	.632	.335	-.294	.491
Over 65 & Living Alone	.638	-.237	.625	-.221	.623	.594	-.302	-.248
Low Income	.799	.246	-.011	-.237	.899	-.039	-.049	.050
Limited English Proficiency	.350	.318	-.098	.655	.827	-.111	.102	-.260
Percent Vegetation	.173	-.867	-.170	.285	-.065	.454	.681	-.018
Percent Urban	-.033	.917	.116	-.228	.223	-.528	-.579	.032
Variance Explained	33.86%	22.60%	14.07%	10.93%	40.44%	17.70%	12.48%	8.31%
Cumulative Variance Explained		56.47%	70.55%	**81.47%**		58.13%	70.61%	**78.91%**

Statistically significant relationships are shown in black

fourth components were characterized as being mostly indicative of environmental vulnerability, while the second and third components were characterized as being more indicative of sociodemographic vulnerability. In Minneapolis, the first and second components were characterized as being indicative of sociodemographic vulnerability, while the third and fourth components were characterized as being indicative of environmental vulnerability.

The sum of the four recoded principal components was used to generate the final, comprehensive heat vulnerability index. The resulting heat vulnerability indices were slightly different for each city: index values for Atlanta ranged from 10 for lowest vulnerability to 20 for highest vulnerability (Figure 9), while index values for Minneapolis ranged from 10 for lowest vulnerability to 21 for highest vulnerability (Figure 10).

In Atlanta, the block groups with higher vulnerability scores are generally located in the southern and western parts of the city, while those with the lowest vulnerability scores tend to be located to the north and, to a lesser extent, the east. This pattern is not universally true, however; based on the heat vulnerability index, three of the top five most vulnerable block groups are located in northern areas of the city. In contrast to Atlanta, the spatial pattern of the most vulnerable block groups in Minneapolis is relatively concentrated.

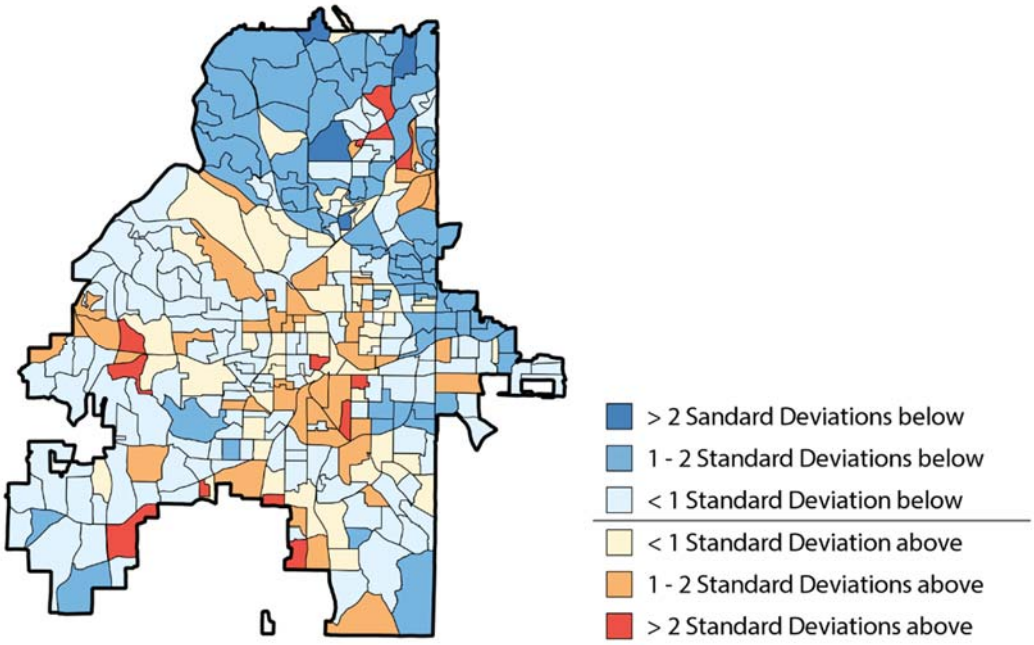

Figure 9: Heat Vulnerability Index for Atlanta

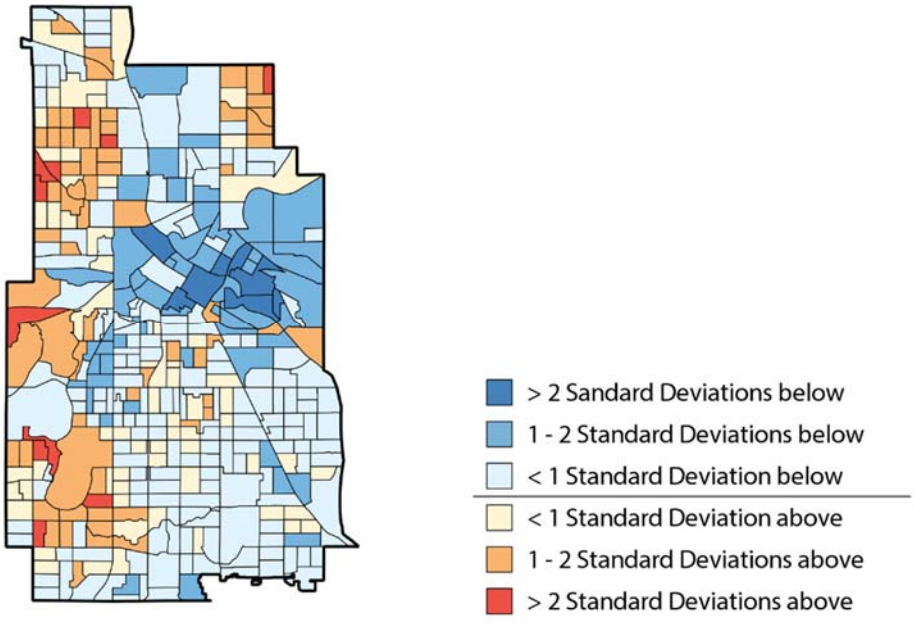

Figure 10: Heat Vulnerability Index for Minneapolis

Whereas highly vulnerable block groups are located almost exclusively in the downtown area, those found to be least vulnerable are positioned to the northeast, northwest, and southwest around the urban periphery.

Figure 11 highlights the spatial distribution and properties of the block groups that received the five highest and lowest cumulative vulnerability scores in each city. Because the most vulnerable block groups can be quite geographically dispersed—as is true in Atlanta, for example—information regarding areas where block groups with similar scores are clustered together can be used by public officials to prioritize policies and employ resources more efficiently. Nevertheless, mapping raw vulnerability scores is beneficial as well, insofar as it may illuminate areas with extreme values that are not necessarily part of a statistically significant cluster.

4.2.3 Spatial Autocorrelation of Vulnerabilities

In order to identify the statistically significant clusters of vulnerable block groups in the cities, LISA was calculated for the sum of the principal components as well as for each component individually. The statistically significant results for the City of Atlanta are shown in Figure 12.

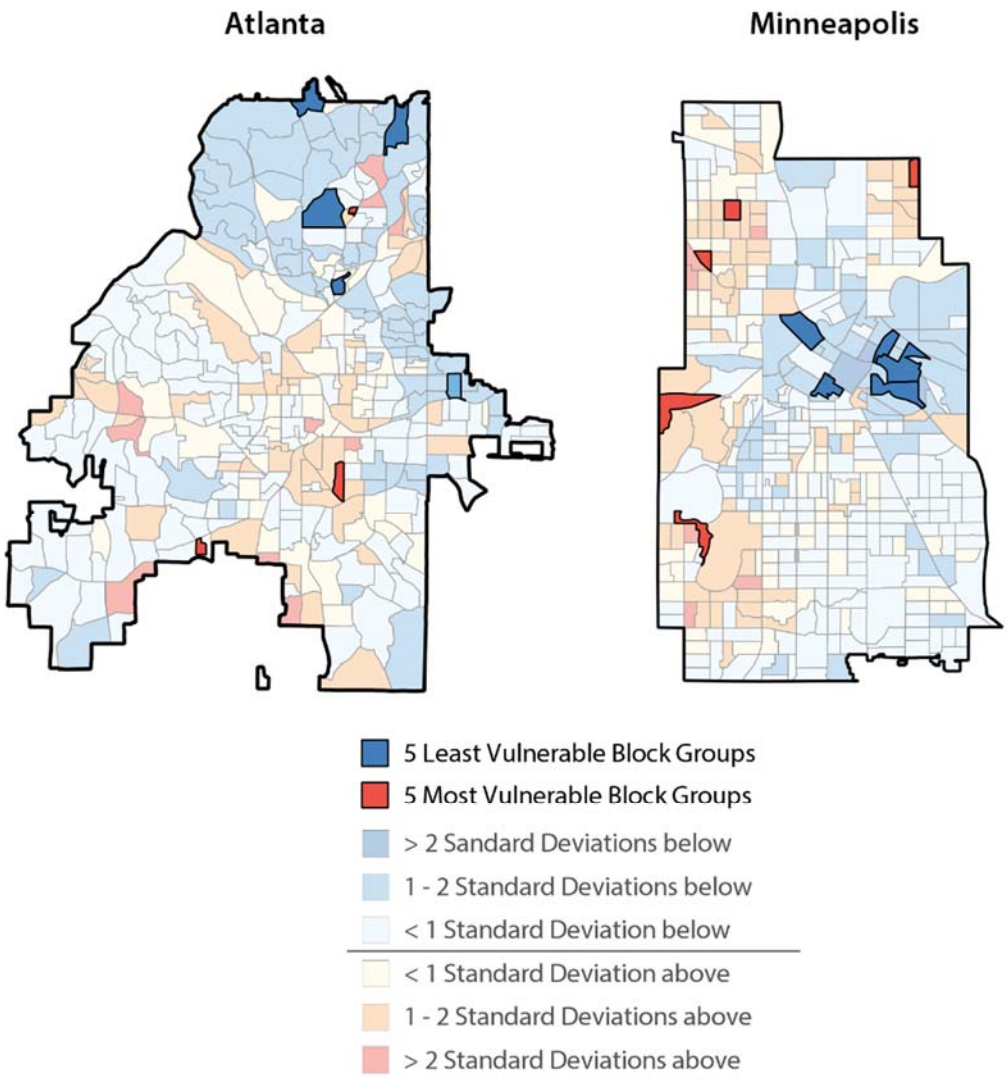

Figure 11: Most and Least Vulnerable Block Groups

The four components extracted for Atlanta captured 81.47% of the cumulative variance in the original data. The first component—interpreted as being indicative of environmental vulnerability—exhibited intense clustering of high vulnerability tracts in the downtown and midtown areas, with lower vulnerability clusters concentrated to the north

and west of downtown along the Chattahoochee River. This was expected, and is likely driven by the relative proportion of vegetative cover and urban surface materials present in those areas. The clusters of low vulnerability block groups to the east and southwest of downtown Atlanta in component four seem to be consistent, at least to some extent, with elevation.

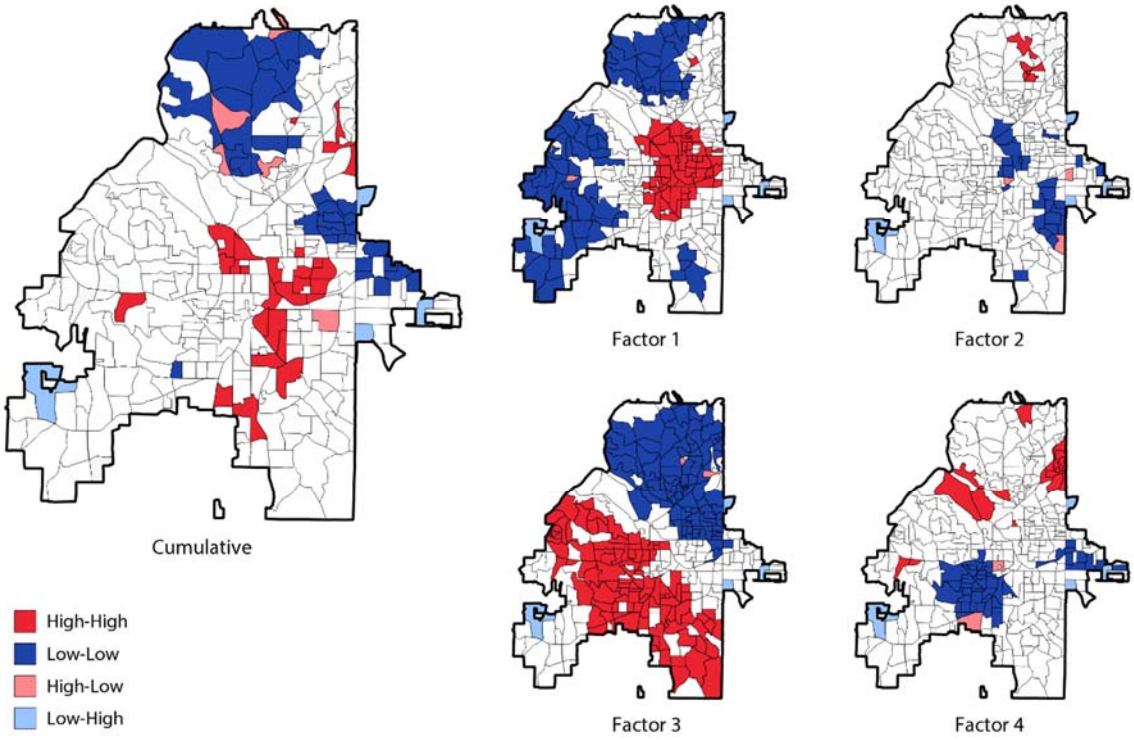

Figure 12: Spatial Autocorrelation of Vulnerability Components for Atlanta

Interestingly, the third component—interpreted as signifying sociodemographic vulnerability—exhibited a distinct, vertical banded pattern, with large clusters of block groups

with high-high and low-low autocorrelation arranged from northwest to southeast across the city. The configuration of block groups shown as highly vulnerable corresponds well with areas in western and southern Atlanta that are generally home to more low income and minority populations, while the areas of low vulnerability in the north of the city tend to comprise higher income populations. In fact, the stark divide between the high-high and low-low clusters in component three mirrors a historic railroad line in the city. The areas in northern parts of Atlanta shown as high vulnerability in the second component are likely categorized as such due to the proportion of the population over age 65.

The linear combination of the principal components yielded less uniform, yet substantial, clusters of high and low heat-vulnerable block groups in Atlanta. A majority of the block groups in the downtown area appear to be in high cumulative vulnerability clusters, while many of the low vulnerability block groups are located in northern Atlanta. This is most similar to what was observed in the first and third components, characteristic of environmental and sociodemographic vulnerability, respectively.

The statistically significant results for the City of Minneapolis are shown in Figure 13. The four principal components extracted for Minneapolis collectively explained 78.91% of the variance in the original data. The first component—interpreted as representing sociodemographic vulnerability—revealed substantial clusters of highly vulnerable block groups in the downtown area, as well as to the northwest along the Mississippi River. These two

areas are home to a comparatively large amount of the city's low income and minority residents. Similarly, both sections of the city also have sizeable immigrant populations, who may potentially lack proficiency with the English language.

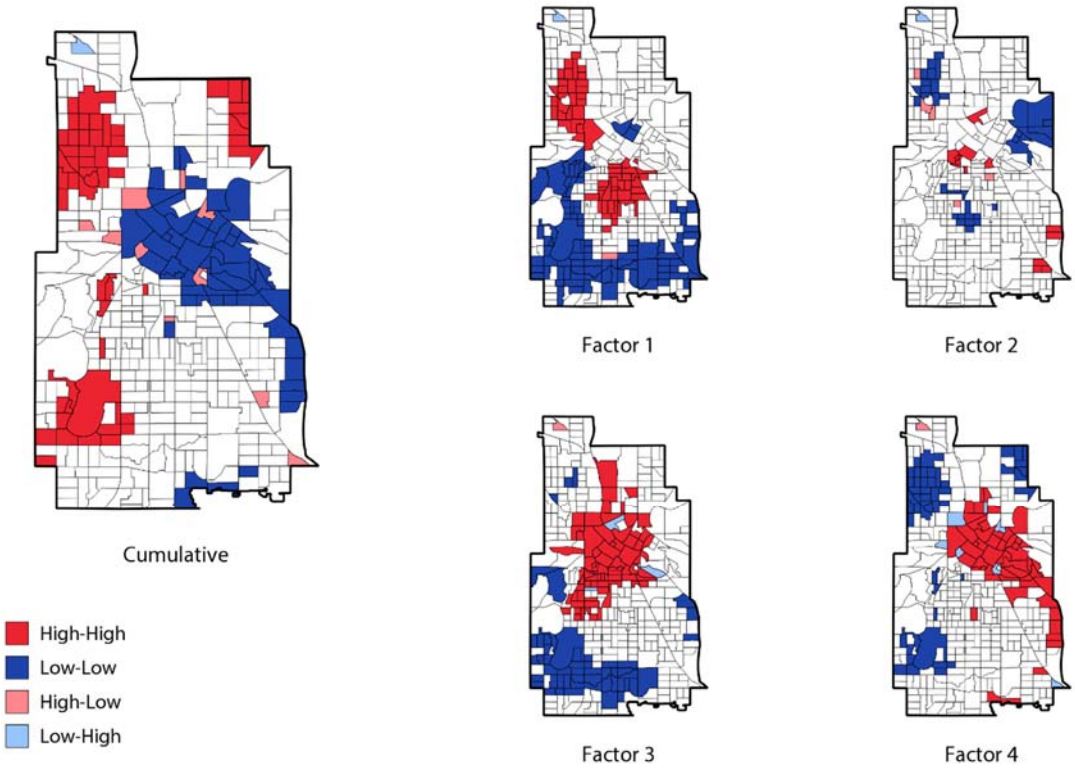

Figure 13: Spatial Autocorrelation of Vulnerability Components for Minneapolis

The third and fourth principal components in Minneapolis—interpreted as being indicative of environmental vulnerability—exhibit nearly identical spatial patterns: clusters of highly vulnerable block groups are concentrated in the downtown areas of the city, with low

vulnerability clusters at the urban periphery. This was also observed in Atlanta, and is largely attributable to the relative proportion of vegetation and urban surface materials present in the areas.

Minneapolis demonstrated a greater amount of spatial autocorrelation of cumulative vulnerability than was displayed by Atlanta. Here, a large cluster of highly vulnerable block groups encompasses the downtown area as well as the areas directly to the north and east, while many of the lower vulnerability block groups are located in a cluster in the southwestern region of the city.

4.3 SPATIAL CORRELATION

Bivariate Moran's I was used to measure, for each grid cell, the spatial correlation between the average heat vulnerability score in that cell and the average surface temperature in neighboring grid cells. The resulting Bivariate LISA value for the City of Atlanta was equal to 0.3247, while the corresponding value for the City of Minneapolis was equal to 0.4006. The outcomes for both cities indicate moderately strong positive correlation exists between elevated temperature and comprehensive vulnerability to heat across the entire urban area, though this relationship is stronger in Minneapolis. The subsequent cluster maps for Atlanta and Minneapolis are shown below (Figures 14 and 15, respectively).

Expectedly, the downtown and midtown areas in Atlanta exhibit high-high spatial correlation. Clusters of cells with high values are also found to the northeast and northwest, connected to the midtown area by linear strands which seem to mirror major interstates. In these areas, policies that offer the co-benefit of reducing vulnerability as well as decreasing temperature should be prioritized. Large groups of low-low clusters are located in northern and southwestern Atlanta, with two smaller clusters directly south of downtown. Smaller clusters of cells categorized as high-low—highly vulnerable and surrounded by low temperature values—are dispersed across the southern, southwestern, and western areas of the city. This is in accordance with the maps showing spatial correlation of vulnerabilities (Figure 12) and surface temperature estimates (Figure 8).

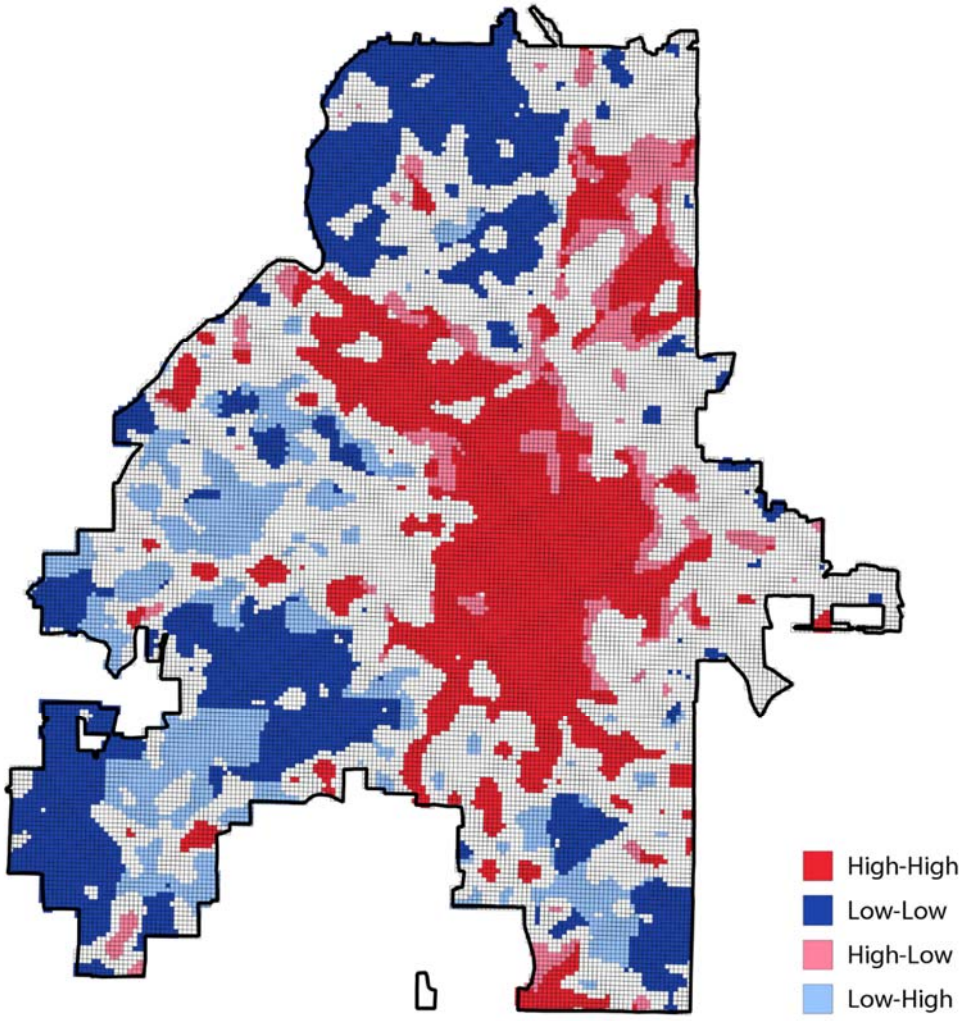

Figure 14: Spatial Correlation between Vulnerability and Temperature in Atlanta

Similar to Atlanta, the areas of high-high clustering in Minneapolis are concentrated in and around the downtown core, with additional clusters to the north crossing over the Mississippi River. Again, policies in these areas can and should be designed with regard to reducing both heat and vulnerability. Areas with low vulnerability surrounded by relatively low temperatures are scattered around the urban periphery, with the largest concentration

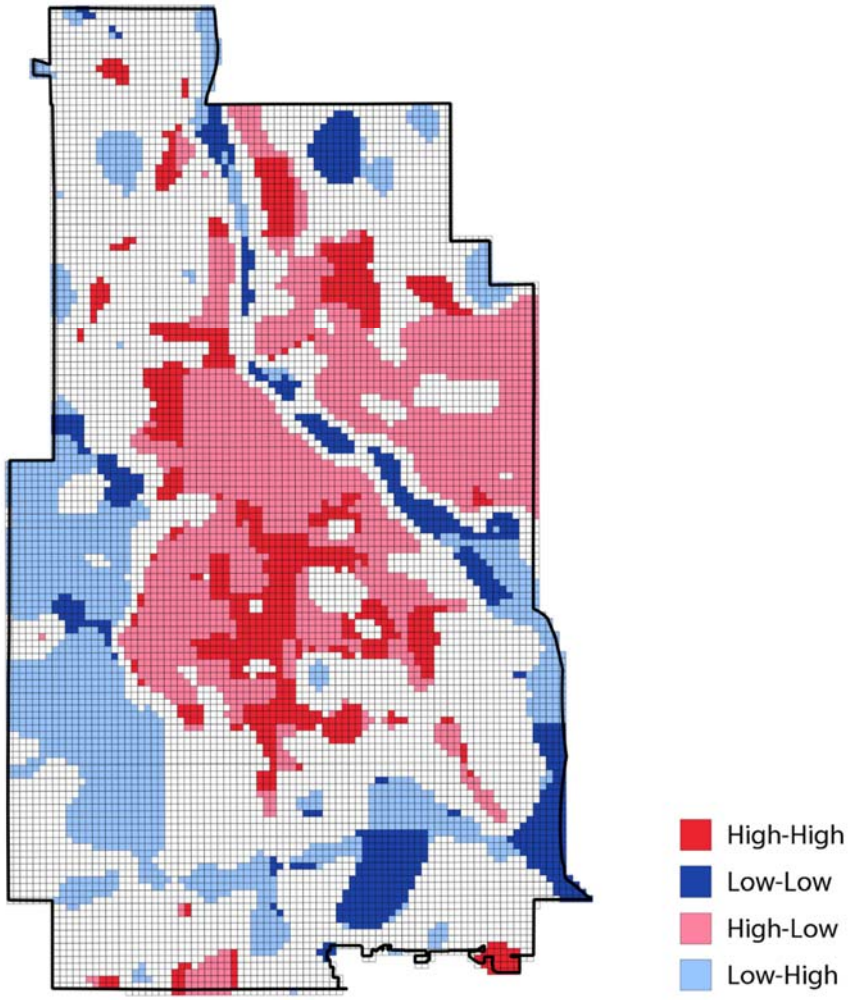

Figure 15: Spatial Correlation between Vulnerability and Temperature in Minneapolis

in the southeastern corner of the city. A majority of the areas shown as having high-low correlation are located over water features—this coheres with the satellite overpass time (11:48 a.m.) and the ability of water to store and retain heat energy during the day.

CHAPTER V

RECOMMENDATIONS

A central goal of this work has been to provide a better understanding of the spatial and substantive relationships between temperature and vulnerability across the urban landscape. Facing an exceedingly critical challenge with increasingly limited resources, cities will likely find the most successful approaches to reducing the negative health consequences of heat to be those that exploit the correlation among and co-location between temperature and vulnerability. The interaction between these phenomena offers distinct opportunities for co-benefit from well-designed and targeted strategies.

The previous chapters have detailed the background and rationale underlying this thesis, as well as presented the study's results that support the presence of reasonably strong spatial and substantive correlation both between the different elements of heat vulnerability and between urban temperature and comprehensive vulnerability to heat in the cities of Atlanta and Minneapolis. This chapter translates those results into practical recommendations for municipalities confronted with the impending growth of at-risk populations and warmer temperatures in the near future.

5.1 A COMPREHENSIVE APPROACH TO HEAT VULNERABILITY

While some cities have taken steps to identify the places where populations most at-risk to the health consequences of heat reside—though, at present, the practice is far from universal—the concept of vulnerability used to do so often includes only social and demographic characteristics and lacks those describing the built environment. In both Atlanta and Minneapolis, comprehensive heat vulnerability exhibited different spatial patterns and correlations than what was demonstrated by either of the sociodemographic or environmental vulnerability components individually. A limitation of this current practice, then, is the failure to examine different vulnerabilities collectively across space. Considerations of at-risk populations based only on social and demographic elements will not capture the true nature of vulnerability throughout the city; thus, policies aimed at reducing the vulnerability of city residents without consideration of the interrelated environmental factors will fail to do so accurately or completely. A comprehensive approach to heat vulnerability, on the other hand, can better inform local policies and emergency response efforts, and help ensure more efficient allocation of resources before, during, and after heat events.

5.1.1 Understanding the Interactions between Elements of Vulnerability

A comprehensive approach to heat vulnerability necessitates an understanding of the nature and direction of relationships between distinct vulnerability elements. In this analysis, significant associations between variables of different vulnerability components were

identified in both cities; a majority of the sociodemographic risk factors were positively correlated with the land cover factors representing environmental risk. City planners and public health officials can develop adaptive mitigation policies that capitalize on these relationships, as well as spatial ones, and offer opportunities for co-benefit among the types of heat vulnerability. Several of the strategies to mitigate heat with corresponding opportunities to reduce vulnerability are discussed in Section 5.2 below.

Importantly, a notable exception to the above relationship was identified in both cities included this study: a negative association existed between the population over 65 and land cover elements of environmental vulnerability. This suggests that land cover-based strategies to mitigate heat will likely fail to provide co-benefits for the elderly. This type of information is valuable for planners and health officials in that it highlights populations for whom more specific policies should be designed.

5.2 STRATEGIES TO MANAGE URBAN HEAT AND ENVIRONMENTAL VULNERABILITY

Strategies to abate heat at the urban and suburban scale are ultimately derived from the ways in which the built environment interacts with and expends thermal energy. Accordingly, these approaches are largely focused on manipulating the physical properties of cities to decrease the amount of heat present near Earth's surface. While additional climate management policies concern improving energy efficiency to reduce waste heat in cities,

the following discussion is primarily concentrated on land cover-based interventions aimed at cooling the built environment.

When considering these policies, a place-based approach is imperative; this includes attention to both regional- and local-scale processes and the environments in which they function. At the regional scale, the suite of strategies available for heat abatement differs for various climatic regions of the country. For example, strategies to mitigate heat through extensive urban reforestation are less appropriate in the arid environments that typify the southwest, but more appropriate for naturally forested environments in the southeast. Instead, strategies implemented in the southwest should take advantage of the abundance of solar radiation received at Earth's surface.

At the local scale, attention must be paid to additional characteristics of the built environment as well as the physical attributes of land cover. Urban morphology, for example, may render less effective a policy aimed at reflecting heat energy if it inhibits the amount of solar radiation incident upon a given surface. In this case, introducing live vegetation onto the surface will likely be more successful at decreasing local temperatures than a strategy of albedo enhancement.

For cities that find vulnerable populations to be positively correlated with environmental exposures, the strategies to reduce heat discussed below can be used to address sociodemographic vulnerability as well.

5.2.1 Urban Greening

The first approach to local heat management involves the augmentation of vegetative cover throughout urban environments. The strategies discussed below work to lower the temperature of cities primarily by increasing the amount of evaporative cooling occurring at or near the surface.

5.2.1.1 Urban Reforestation

Urban reforestation is perhaps the most powerful heat abatement strategy available to cities today. By shading local surfaces and performing evapotranspiration—a natural cooling mechanism that dissipates heat energy into the atmosphere—trees can significantly decrease the temperature of an area. Though the precise reduction in temperature is dependent upon local variables, urban trees have been found to cool the environment by as much as 1.8 to 3.6°F under normal circumstances [60], and by more than 12°F under extreme heat circumstances [71].

During urban expansion, deforestation often occurs in favor of the development of the built environment; this process is a significant driver of heat island formation. Thus, it is reasonable to expect that a reintroduction of tree canopy into the urban and regional environments can mitigate, at least to some extent, the heat island effect. Inherent within

this strategy is the termination of deforestation, both in the city and throughout the greater metropolitan region.

Urban reforestation, including planting street trees in the public right-of-way and on private residential lots, provides additional benefits beyond the reduction of heat. Coupled with efforts to conserve existing trees, expansion of the urban tree canopy can help to lower energy consumption and cost, increase stormwater retention and decrease runoff, reduce air pollution, and enhance quality of life for city residents. As Stone concludes, "for urban governments serious about the public health threats of climate change, reforestation of metropolitan regions, including dense inner-city cores, offers perhaps the least costly and most effective strategy available to manage extreme heat" [57, p. 102].

Tree ordinances are one of the most prevalent mechanisms through which municipalities protect and regulate the urban tree canopy. These policies typically govern the planting, maintenance, and removal of trees on public property or in the right-of-way, and may extend to trees and shrubs on private land as well.

The City of Atlanta adopted a particularly strong tree ordinance that mandates 'no net loss of trees' owing to development within the city limits. Originally enacted in 1977, Atlanta's tree ordinance requires a permit to remove or otherwise injure any tree on public property as well as any mature tree (that is, one with a diameter at breast height (DBH)

greater than six inches) on private property. Additionally, permit applications must be supplemented with a tree replacement plan, which details the location of trees that will be planted on-site to compensate for vegetation lost during construction, demolition, or redevelopment of a lot. The number of replacement trees must meet or exceed the number of trees lost, or else recompense fees must be paid into the city's Tree Trust Fund.

5.2.1.2 Green Roofs and Green Walls

Together, green roofs and green walls represent a heat mitigation strategy whereby a layer of live vegetation, grown on either a building rooftop or an exterior wall, supplies shade and performs evapotranspiration aimed at cooling local air and reducing energy demand. This strategy is well-suited for cities focused on managing urban hot spots in high density developed areas, as it provides a means of incorporating vegetation into areas that lack available open space at the surface. With little upkeep, green roofs and green walls offer extensive advantages beyond cooling the local environment, including "reduction of [stormwater] runoff ..., improved energy performance of buildings, reduced noise and air pollution, health improvements, better amenity value, increased property values, [and] improved biodiversity" [13, p. 55]. Although additional funding and maintenance is required, intensive green roofs—rooftop parks and gardens, for example—may provide still further benefit by serving as an amenity to the general public.

In 2009, the City of Toronto passed a Green Roof bylaw mandating the installation of green roofs on all new commercial, residential, and institutional development or structural additions with a gross floor area (GFA) greater than 2,000 square meters. The bylaw requirements for percent coverage of green area are in direct relation to the size of the building, ranging from 20% coverage for buildings with a minimum GFA of 2,000 square meters to 60% coverage for buildings with a minimum GFA greater than 20,000 square meters. If a building does not meet the percent coverage requirement for green roofs, cash in lieu of construction must be remunerated to the Eco-Roof Incentive Program, which provides financial incentives for the installation of green and cool roofs in the City of Toronto.

5.2.2 Increasing the Albedo of Urban Surfaces

The second approach to local heat management involves increasing the albedo of urban surfaces. As discussed in Chapter II, albedo dictates the proportion of incident radiation reflected—and, consequently, the proportion absorbed and re-emitted—by a surface. Raising the albedo of urban surfaces increases the amount of heat energy reflected back into the atmosphere, thereby limiting the amount present at Earth's surface.

That albedo enhancement is one of the most common approaches used to cool cities today is primarily due to its relatively low cost and ease of implementation. On average, roofs and pavements constitute between 50 and 70% of impervious surfaces in cities [1]; modification of these surfaces therefore represents a considerable opportunity to cool local

temperatures. Strategies that increase the albedo of existing structures and those that incorporate it into future development are straightforward and similar in nature. These can entail the resurfacing of existing impervious surfaces such as roofs and pavement with materials that are lightly-colored and more reflective, or can entail the inclusion of lightly-colored, reflective materials in the construction of new roads and buildings.

In December 2013, Los Angeles became the first major city in the United States to mandate roof albedo in the Municipal Building Code. Known as the "Cool Roof Ordinance," the regulation requires roofing materials on all new residential development to meet certain surface reflectance and thermal emittance standards according to roof slope. Cool roofs are a popular example of albedo enhancement, and have been shown to remain approximately 60°F cooler than conventional surfaces during extreme heat events [56]. By decreasing the temperature of the building envelope, cool roofs offer additional advantages such as reduced energy demand, lower cooling cost, and decreased greenhouse gas emissions as well.

Furthermore, increasing surface albedo also has co-benefits for the health of city residents. As noted by Harlan and Ruddell (2011), albedo enhancements can help reduce heat-related and respiratory illnesses, and improve comfort of both the indoor and outdoor urban environments [21]. In areas where vulnerable populations coincide with local hot spots, programs to increase surface reflectivity will likely prove cost effective and successful.

While increasing surface albedo will undoubtedly help to cool local temperatures and allay heat-related health risks, this policy will be less effective in areas of low density development with more pervious land cover that cannot easily be modified [55]. This is also true in areas where tree canopy or other vegetation obscures the surfaces with increased albedo from receiving radiation. Even in high density downtown cores, the urban form has significant implications for the transfer of heat that may render a different strategy more effective [66].

5.3 STRATEGIES TO ADDRESS SOCIODEMOGRAPHIC VULNERABILITY TO HEAT

While the strategies to reduce environmental vulnerability are focused on the causes of elevated temperatures, the strategies that address sociodemographic vulnerability are focused more on the individuals that are affected by them. More so than the approaches to reduce local temperature discussed above, these strategies must be sensitive to different populations, locations, and cultures, and therefore vary widely in quality and style. As such, specific policies are not discussed in depth here—instead, a brief summary is given of more general policies that may be used to address heat vulnerability in populations less likely to reap the benefits of decreased temperatures, or in populations found to be less co-located with extreme heat.

Each year, extreme heat is the most destructive climate-related phenomenon to human life [44], yet a general perception exists that heat events are less of a serious threat to human health than other natural disasters. Raising awareness of the health dangers associated with extreme heat can help individuals make more informed decisions before and during periods of higher temperatures. Efforts to engage communities in a discussion of heat vulnerability and adaptation measures "will not only enhance their resilience to climate stressors, but will likely increase their ability to cope with a wide range of other societal issues" [11, p. 502]. Furthermore, community involvement in adaptation planning can be of great utility by ensuring messages targeted to individual populations are appropriate and direct [11].

5.4 INTRODUCING A SPATIAL COMPONENT INTO HEAT-HEALTH VULNERABILITY

Incorporating a spatial component into the greater discussion of heat-health vulnerability can add significant value to adaptation efforts. This may be considered analogously with a distinct appreciation for scale; specifically, what is the most appropriate scale at which to address climate change? Many current attempts center on reducing greenhouse gas emissions through international policy frameworks. Focusing attention almost exclusively on global processes, however, ignores both the causes and effects of climate change where a majority of the population lives. Instead, local policies to address heat risk in cities

have the advantage of being flexible, practical, and culturally-, financially-, and politically-appropriate.

The public health value added from a geographic perception in analyses similar to those performed herein is most thoroughly expressed by Hess et. al (2008):

> *[A] focus on place emphasizes the local nature of both exposures and response, and it brings attention to environmental changes where the motivation to address them is strongest. Emphasizing place highlights climate change's effects where they are most acutely felt, where local strengths are best understood, where place attachment can be leveraged most effectively, and where residents will reap the benefits of adaptive measures promoting sustainability and livable communities. (p. 476)*

Introducing a spatial component into heat-health assessments can improve cities' understanding of issues that directly impact the well-being of their residents. At best, a focus on place can advise the scales at which city resources are most efficiently deployed; at worst, disregarding the spatial factor underlying heat risk may prove costly to human life. While this strategy alone will not cool local temperatures or reduce sociodemographic vulnerability, it can help elucidate some of the otherwise enigmatic challenges that define urban climate change. Ultimately, though implicit in all of the recommendations above, an explicit consideration of place can benefit mitigation and adaptation efforts currently underway in urban areas and inform those in the future.

CHAPTER VI

CONCLUSION

The purpose of this work has been to advance current understanding of the spatial relationship between local hot spots and vulnerability to heat across the urban environment. As cities confront the challenge of managing both warming temperatures and urban population growth simultaneously, with increasingly less resources available with which to do so, the most efficient mitigation policies will be those that take advantage of associations between the social and physical environments. An understanding of where these opportunities exist therefore becomes invaluable to policy makers, public health officials, and city planners alike.

6.1 SUMMARY OF FINDINGS

A key outcome of this research, comprehensive heat vulnerability was shown to exhibit different spatial patterns and correlations to temperature than was demonstrated by either the sociodemographic or environmental vulnerability components individually. This suggests analyses of sociodemographic vulnerability that do not consider environmental components fail to accurately capture the true nature of the phenomenon across space. A

comprehensive approach to heat vulnerability can better inform local policies and emergency response efforts.

These findings also reveal the interactions between variables of the sociodemographic and environmental vulnerability components. Planners and public health officials can use this detailed information to design land cover-based heat mitigation policies that capitalize on the positive relationships and offer opportunities for co-benefit among the types of vulnerability. The negative relationships, on the other hand, must be considered independently, and specific policies should be tailored with respect to the population and location being addressed.

Ultimately, the results of this analysis reveal a moderately strong, positive spatial correlation between temperature and comprehensive heat vulnerability across the urban environment. Both Atlanta and Minneapolis displayed a similar spatial pattern, with areas of high vulnerability and high temperature clustered in the downtown area and areas of low vulnerability and low temperature dispersed at the urban periphery.

6.2 FUTURE WORK

First and foremost, future applications of this work should endeavor to estimate near-surface air temperature as was initially intended here. To do so accurately would require a

larger and more evenly distributed sample of temporally-consistent temperature observations at the urban scale. Currently, such a network does not exist—or was not identified throughout the course of this study—in the United States. Nonetheless, air temperature would provide more accurate results regarding the association between heat and human health.

Another prospective direction of this work is to examine the temporal relationship between local hot spots and vulnerability to heat. A possible analysis of this nature could evaluate whether risk in a city is increasing or decreasing over time, or, potentially, whether populations are becoming more or less vulnerable over time. Future work may also examine the spatial concentration and/or diffusion of vulnerability components.

Finally, this analysis should be conducted in additional cities around the country. Not only would doing so provide more robust evidence and authentication for the relationships found in this work, it would also supply more cities with detailed information regarding the spatial patterns of temperature and vulnerability to heat throughout the urban landscape. Since the most successful strategies will be those aimed at simultaneously reducing both local temperatures and vulnerability to heat, this can serve as an important tool for local governments to manage the relationship between heat and human health. As cities begin to recognize the implications of climate change at the local scale, they must also contend with the growth of vulnerable populations and the decline of resources with which to manage

either. The findings of this analysis can inform the most efficient ways to overcome this challenge, and can help cities to become healthier, more livable places in the future.

REFERENCES

[1] Akbari, Hashem, and Leanna Shea Rose. "Urban Surfaces and Heat Island Mitigation Potentials." *Journal of the Human-Environment System* 11, no. 2 (2008): 85-101.

[2] Basu, R. "Relation between Elevated Ambient Temperature and Mortality: A Review of the Epidemiologic Evidence." *epidemiologic reviews* 24, no. 2 (2002): 190-202.

[3] Basu, R., and B. D. Ostro. "A Multicounty Analysis Identifying the Populations Vulnerable to Mortality Associated with High Ambient Temperature in California." *American Journal of Epidemiology* 168, no. 6 (2008): 632-637.

[4] Basu, R., and J. M. Samet. "Relation between Elevated Ambient Temperature and Mortality: A Review of the Epidemiologic Evidence." *Epidemiologic Reviews* 24, no. 2 (2002): 190-202.

[5] Bohling, G. "Kriging." Lecture in Data Analysis for Engineering and Natural Science at Kansas University, Lexington, KY., October 19, 2005.

[6] Cardona, O.D., M.K. van Aalst, J. Birkmann, M. Fordham, G. McGregor, R. Perez, R.S. Pulwarty, E.L.F. Schipper, and B.T. Sinh, 2012: Determinants of risk: exposure and vulnerability. In: *Managing the Risks of Extreme Events and Disasters to Advance Climate Change Adaptation* [Field, C.B., V. Barros, T.F. Stocker, D. Qin, D.J. Dokken, K.L. Ebi, M.D. Mastrandrea, K.J. Mach, G.-K. Plattner, S.K. Allen, M. Tignor, and P.M. Midgley (eds.)]. A Special Report of Working Groups I and II of the Intergovernmental Panel on Climate Change (IPCC). Cambridge University Press, Cambridge, UK, and New York, NY, USA, pp. 65-108.

[7] Cohen, Jonathan, R. Webster, and M. A. Oliver. "Statistical Methods in Soil and Land Resource Survey." *Technometrics* 34, no. 4 (1992): 497.

[8] Cressie, Noel A. C. *Statistics for spatial data*. New York: Wiley, 1993.

[9] Curriero, F. C. "Temperature and Mortality in 11 Cities of the Eastern United States." *American Journal of Epidemiology* 155, no. 1 (2002): 80-87.

[10] Dole, R., M. Hoerling, J. Perlwitz, J. Eischeid, P. Pegion, T. Zhang, X.-W. Quan, T. Xu, and D. Murray. “Was there a Basis for Anticipating the 2010 Russian Heat Wave?” Geophysical Research Letters 38, no. 6 (2011).

[11] Ebi, Kristie L., and Jan C. Semenza. "Community-Based Adaptation to the Health Impacts of Climate Change." *American Journal of Preventive Medicine* 35, no. 5 (2008): 501-507.

[12] Electricity Consumers Resource Council. "The Economic Impacts of the August 2003 Blackout." Working paper, February 9, 2004.

[13] Field, C.B., V.R. Barros, K.J. Mach, M.D. Mastrandrea, M. van Aalst, W.N. Adger, D.J. Arent, J. Barnett, R. Betts, T.E. Bilir, J. Birkmann, J. Carmin, D.D. Chadee, A.J. Challinor, M. Chatterjee, W. Cramer, D.J. Davidson, Y.O. Estrada, J.-P. Gattuso, Y. Hijioka, O. Hoegh-Guldberg, H.-Q. Huang, G.E. Insarov, R.N. Jones, R.S. Kovats, P. Romero Lankao, J.N. Larsen, I.J. Losada, J.A. Marengo, R.F. McLean, L.O. Mearns, R. Mechler, J.F. Morton, I. Niang, T. Oki, J.M. Olwoch, M. Opondo, E.S. Poloczanska, H.-O. Pörtner, M.H. Redsteer, A. Reisinger, A. Revi, D.N. Schmidt, M.R. Shaw, W. Solecki, D.A. Stone, J.M.R. Stone, K.M. Strzepek, A.G. Suarez, P. Tschakert, R. Valentini, S. Vicuña, A. Villamizar, K.E. Vincent, R. Warren, L.L. White, T.J. Wilbanks, P.P. Wong, and G.W. Yohe, 2014: Technical Summary. In: *Climate Change 2014: Impacts, Adaptation, and Vulnerability. Part A: Global and Sectoral Aspects. Contribution of Working Group II to the Fifth Assessment Report of the Intergovernmental Panel on Climate Change* [Field, C.B., V.R. Barros, D.J. Dokken, K.J. Mach, M.D. Mastrandrea, T.E. Bilir, M. Chatterjee, K.L. Ebi, Y.O. Estrada, R.C. Genova, B. Girma, E.S. Kissel, A.N. Levy, S. MacCracken, P.R. Mastrandrea, and L.L. White (eds.)]. Cambridge University Press, Cambridge, United Kingdom and New York, NY, USA, pp. 1-76.

[14] Forinash, Kyle. *Foundations of environmental physics: understanding energy use and human impacts*. Washington, D.C.: Island Press, 2010.

[15] Frumkin, Howard, Anthony J. McMichael, and Jeremy J. Hess. "Climate Change and the Health of the Public." *American Journal of Preventive Medicine* 35, no. 5 (2008): 401-402.

[16] Frumkin, Howard, and Anthony J. McMichael. "Climate Change and Public Health." *American Journal of Preventive Medicine* 35, no. 5 (2008): 403-410.

[17] Haines, A, R Kovats, D Campbell, and C Corvalan. "Climate Change and Human Health: Impacts, Vulnerability and Public Health." Public Health 120, no. 7 (2006): 585-596.

[18] Hajat, S., and T. Kosatky. "Heat-related mortality: a review and exploration of heterogeneity." *Journal of Epidemiology & Community Health* 64, no. 9 (2010): 753-760.

[19] Hansen, A. L, P. Bi, P. Ryan, M. Nitschke, D. Pisaniello, and G. Tucker. "The effect of heat waves on hospital admissions for renal disease in a temperate city of Australia." International Journal of Epidemiology 37, no. 6 (2008): 1359-1365.

[20] Hansen, Alana, Peng Bi, Monika Nitschke, Philip Ryan, Dino Pisaniello, and Graeme Tucker. "The Effect of Heat Waves on Mental Health in a Temperate Australian City." Environmental Health Perspectives 116, no. 10 (2008): 1369-1375.

[21] Harlan, Sharon L, and Darren M Ruddell. "Climate change and health in cities: impacts of heat and air pollution and potential co-benefits from mitigation and adaptation." *Current Opinion in Environmental Sustainability* 3, no. 3 (2011): 126-134.

[22] Harlan, Sharon L., Anthony J. Brazel, Lela Prashad, William L. Stefanov, and Larissa Larsen. "Neighborhood Microclimates and Vulnerability to Heat Stress." *Social Science & Medicine* 63, no. 11 (2006): 2847-2863.

[23] Hess, J.J., J.N. Malilay, and A.J. Parkinson. "Climate change: The importance of place." *American Journal of Preventive Medicine* 35, no. 5 (2008): 468-478.

[24] Howard, Luke. *The climate of London deduced from meteorological observations made in the metropolis and at various places around it*. 2nd ed. London: Harvey and Darton, 1833.

[25] Huang, Ganlin, Weiqi Zhou, and M.l. Cadenasso. "Is everyone hot in the city? Spatial pattern of land surface temperatures, land cover and neighborhood socioeconomic characteristics in Baltimore, MD." *Journal of Environmental Management* 92, no. 7 (2011): 1753-1759.

[26] IPCC, 2014: Summary for policymakers. In: *Climate Change 2014: Impacts, Adaptation, and Vulnerability. Part A: Global and Sectoral Aspects. Contribution of Working Group II to the Fifth Assessment Report of the Intergovernmental Panel on Climate Change* [Field, C.B., V.R. Barros, D.J. Dokken, K.J. Mach, M.D. Mastrandrea, T.E. Bilir, M. Chatterjee, K.L. Ebi, Y.O. Estrada, R.C. Genova, B. Girma, E.S. Kissel, A.N. Levy, S. MacCracken, P.R. Mastrandrea, and L.L.White (eds.)]. Cambridge University Press, Cambridge, United Kingdom and New York, NY, USA, pp. 1-32.

[27] Johnson, Daniel P, Jeffrey S Wilson, and George C Luber. "Socioeconomic indicators of heat-related health risk supplemented with remotely sensed data." *International Journal of Health Geographics* 8, no. 1 (2009): 57.

[28] Johnson, Daniel P., Austin Stanforth, Vijay Lulla, and George Luber. "Developing an applied extreme heat vulnerability index utilizing socioeconomic and environmental data." *Applied Geography* 35, no. 1-2 (2012): 23-31.

[29] Kalkstein, Laurence S., and Robert E. Davis. "Weather and Human Mortality: An Evaluation of Demographic and Interregional Responses in the United States." *Annals of the Association of American Geographers* 79, no. 1 (1989): 44-64.

[30] Kilbourne, E. M. "Risk factors for heatstroke. A case-control study." *JAMA: The Journal of the American Medical Association* 247, no. 24 (1982): 3332-3336.

[31] Klinenberg, Eric. *Heat wave: a social autopsy of disaster in Chicago*. Chicago: University of Chicago Press, 2002.

[32] Knowlton, Kim, Miriam Rotkin-Ellman, Galatea King, Helene G. Margolis, Daniel Smith, Gina Solomon, Roger Trent, and Paul English. "The 2006 California Heat Wave: Impacts on Hospitalizations and Emergency Department Visits." *Environmental Health Perspectives* 117 (2008).

[33] Kovats, R. Sari, and Shakoor Hajat. "Heat Stress and Public Health: A Critical Review." *Annual Review of Public Health* 29, no. 1 (2008): 41-55.

[34] Lo, C. P., D. A. Quattrochi, and J. C. Luvall. "Application of high-resolution thermal infrared remote sensing and GIS to assess the urban heat island effect." *International Journal of Remote Sensing* 18, no. 2 (1997): 287-304.

[35] Luber, George, and Michael McGeehin. "Climate Change and Extreme Heat Events." *American Journal of Preventive Medicine* 35, no. 5 (2008): 429-435.

[36] McGeehin, Michael A., and Maria Mirabelli. "The Potential Impacts of Climate Variability and Change on Temperature-Related Morbidity and Mortality in the United States." *Environmental Health Perspectives* 109 (2001): 185.

[37] McMichael, A. "Climate change and human health: Issues and priorities for adaptive strategies and for public health functions," in R Bierbaum, D G Brown, J L McAlpine (ed.), *Coping with Climate Change: National Summit*, Ann Arbor: Island Press, 2008.

[38] McMichael, Anthony J, Rosalie E Woodruff, and Simon Hales. "Climate Change And Human Health: Present and Future Risks." *The Lancet* 367, no. 9513 (2006): 859-869.

[39] McMichael, A. J., and K. B. G. Dear. "Climate change: Heat, health, and longer horizons." *Proceedings of the National Academy of Sciences* 107, no. 21 (2010): 9483-9484.

[40] Mills, Gerald. "Cities as agents of global change." *International Journal of Climatology* 27, no. 14 (2007): 1849-1857.

[41] Oke, T. R. "The energetic basis of the urban heat island," Quarterly Journal of the Royal Meteorological Society, vol. 108, no. 455, 1982.

[42] Oke, T. R. *Boundary layer climates*. Routledge, 1987.

[43] O'Neill, Marie S., Rebecca Carter, Jonathan K. Kish, Carina J. Gronlund, Jalonne L. White-Newsome, Xico Manarolla, Antonella Zanobetti, and Joel D. Schwartz. "Preventing heat-related morbidity and mortality: New approaches in a changing climate." *Maturitas* 64, no. 2 (2009): 98-103.

[44] Patz, J. A. "Hotspots in climate change and human health." *BMJ* 325, no. 7372 (2002): 1094-1098.

[45] Portier CJ, Thigpen Tart K, Carter SR, Dilworth CH, Grambsch AE, Gohlke J, Hess J, Howard SN, Luber G, Lutz JT, Maslak T, Prudent N, Radtke M, Rosenthal JP, Rowles T, Sandifer PA, Scheraga J, Schramm PJ, Strickman D, Trtanj JM, Whung P-Y. 2010. *A Human Health Perspective On Climate Change: A Report Outlining the Research Needs on the Human Health Effects of Climate Change*. Research Triangle Park, NC: Environmental Health Perspectives/National Institute of Environmental Health Sciences. doi:10.1289/ehp.1002272 Available: www.niehs.nih.gov/climatereport

[46] Qin, Z., A. Karnieli, and P. Berliner. "A Mono-window Algorithm for Retrieving Land Surface Temperature from Landsat TM Data and Its Application to the Israel-Egypt Border Region." *International Journal of Remote Sensing* 22, no. 18 (2001): 3719-3746.

[47] Rajasekar, Umamaheshwaran, and Qihao Weng. "Spatio-temporal modelling and analysis of urban heat islands by using Landsat TM and ETM+ imagery." *International Journal of Remote Sensing* 30, no. 13 (2009): 3531-3548.

[48] Reid, Colleen, Marie O'Neill, Carina Gronlund, Shannon Brines, Dan Brown, Ana Diez-Roux, and Joel Schwartz. "Mapping Community Determinants of Heat Vulnerability." *Environmental Health Perspectives* 117 (2009): 1730.

[49] Rhea, Sarah, Amy Ising, Aaron T. Fleischauer, Lana Deyneka, Heather Vaughan-Batten, and Anna Waller. "Using Near Real-Time Morbidity Data to Identify Heat-Related Illness Prevention Strategies in North Carolina." *Journal of Community Health* 37, no. 2 (2012): 495-500.

[50] Robine, Jean-Marie, Siu Lan K. Cheung, Sophie Le Roy, Herman Van Oyen, Clare Griffiths, Jean-Pierre Michel, and Francois Richard Herrmann. "Death toll exceeded 70,000 in Europe during the summer of 2003." *Comptes Rendus Biologies* 331, no. 2 (2008): 171-178.

[51] Roth, M., T. R. Oke, and W. J. Emery. "Satellite-derived urban heat islands from three coastal cities and the utilization of such data in urban climatology." *International Journal of Remote Sensing* 10, no. 11 (1989): 1699-1720.

[52] Semenza, J. "Excess hospital admissions during the July 1995 heat wave in Chicago." *American Journal of Preventive Medicine* 16, no. 4 (1999): 269-277.

[53] Semenza, Jan C., Carol H. Rubin, Kenneth H. Falter, Joel D. Selanikio, W. Dana Flanders, Holly L. Howe, and John L. Wilhelm. "Heat-Related Deaths during the July 1995 Heat Wave in Chicago." *New England Journal of Medicine* 335, no. 2 (1996): 84-90.

[54] Smith, K.R., A. Woodward, D. Campbell-Lendrum, D.D. Chadee, Y. Honda, Q. Liu, J.M. Olwoch, B. Revich, and R. Sauerborn, 2014: Human health: impacts, adaptation, and co-benefits. In: *Climate Change 2014: Impacts, Adaptation, and Vulnerability. Part A: Global and Sectoral Aspects. Contribution of Working Group II to the Fifth Assessment Report of the Intergovernmental Panel on Climate Change* [Field, C.B., V.R. Barros, D.J. Dokken, K.J. Mach, M.D. Mastrandrea, T.E. Bilir, M. Chatterjee, K.L. Ebi, Y.O. Estrada, R.C. Genova, B. Girma, E.S. Kissel, A.N. Levy, S. MacCracken, P.R. Mastrandrea, and L.L. White (eds.)]. Cambridge University Press, Cambridge, United Kingdom and New York, NY, USA, pp. 1-69.

[55] Stone, Brian, Jr. "A Remote Sensing Analysis of Residential Land Use, Forest Canopy Distribution, and Surface Heat Island Formation in the Atlanta Metropolitan Region." PhD diss., Georgia Institute of Technology.

[56] Stone, Brian. "Land Use as Climate Change Mitigation." *Environmental Science & Technology* 43, no. 24 (2009): 9052-9056.

[57] Stone, Brian. *The City and the Coming Climate: Climate Change in the Places We Live*. New York: Cambridge University Press, 2012.

[58] Stone, Brian, Jason Vargo, and Dana Habeeb. "Managing climate change in cities: Will climate action plans work?" *Landscape and Urban Planning* 107, no. 3 (2012): 263-271.

[59] Streutker, D. "Satellite-measured growth of the urban heat island of Houston, Texas." *Remote Sensing of Environment* 85, no. 3 (2003): 282-289.

[60] Taha, H. "Urban Climates and Heat Islands: Albedo, Evapotranspiration, and Anthropogenic Heat." *Energy and Buildings* 25, no. 2 (1997): 99-103.

[61] Tan, Jianguo. "Commentary: People's vulnerability to heat wave." *International Journal of Epidemiology* 37, no. 2 (2008): 318-320.

[62] Tobler, W. R. "A Computer Movie Simulating Urban Growth in the Detroit Region." *Economic Geography* 46 (1970): 234.

[63] Uejio, Christopher K., Olga V. Wilhelmi, Jay S. Golden, David M. Mills, Sam P. Gulino, and Jason P. Samenow. "Intra-urban societal vulnerability to extreme heat: The role of heat exposure and the built environment, socioeconomics, and neighborhood stability." *Health & Place* 17, no. 2 (2011): 498-507.

[64] United States Environmental Protection Agency, "Reducing Urban Heat Islands: Compendium of Strategies," tech. rep., United States Environmental Protection Agency, 2008.

[65] Van De Griend, A. A., and M. Owe. "On the relationship between thermal emissivity and the normalized difference vegetation index for natural surfaces." *International Journal of Remote Sensing* 14, no. 6 (1993): 1119-1131.

[66] Vargo, Jason. "Planning for the New Urban Climate: Interactions of Local Environmental Planning and Regional Extreme Heat." PhD diss., Georgia Institute of Technology.

[67] Vargo, Jason, Dana Habeeb, and Brian Stone. "The importance of land cover change across urban-rural typologies for climate modeling." *Journal of Environmental Management* 114 (2013): 243-252.

[68] Voogt, J.A, and T.R Oke. "Thermal remote sensing of urban climates." *Remote Sensing of Environment* 86, no. 3 (2003): 370-384.

[69] *World urbanization prospects the 2011 revision*. New York: United Nations, 2012.

[70] Zhang, Jinqu, Yunpeng Wang, and Yan Li. "A C++ Program for Retrieving Land Surface Temperature from the Data of Landsat TM/ETM+ Band6." *Computers & Geosciences* 32, no. 10 (2006): 1796-1805.

[71] Zhou, Yan, and J. Marshall Shepherd. "Atlanta's urban heat island under extreme heat conditions and potential mitigation strategies." *Natural Hazards* 52, no. 3 (2010): 639-668.